ANALYSIS OF NEUTRON ENVIRONMENTS IN ADVANCED REACTORS VS. TRIGA REACTOR FOR IN-CORE BEHAVIOR STUDIES

A Thesis

by

GRACE ANN MARCANTEL

Submitted to the Office of Graduate and Professional Studies of
Texas A&M University
in partial fulfillment of the requirements for the degree of

MASTER OF SCIENCE

Chair of Committee,	Pavel V. Tsvetkov
Committee Members,	Karen V. Kirkland
	Michael B. Pate
Head of Department,	Yassin A. Hassan

May 2018

Major Subject: Nuclear Engineering

ABSTRACT

The Fluoride High-Temperature Reactor (FHR) and the Very High-Temperature Reactor (VHTR) are advanced reactor designs in the generation IV class. Advanced reactors operate in more strenuous conditions than older generation II designs which can be detrimental to data collecting equipment; Therefore, equipment must be tested under comparable conditions to simulate how it would respond and operate. This research focuses on computationally altering Texas A&M's TRIGA reactor neutronics using MCNP to compare against advanced reactor neutronics.

Several energy spectrums of interest were collected using MCNP for the FHR and VHTR over the active fuel region, coolant, graphite (in the active core), and graphite reflector. The energy spectrum of the TRIGA's in-core irradiation location was collected with a thermal peak centerline energy (the energy at which the peak is located) considerably lower than the FHR and VHTR in all locations. The in-core irradiation location was altered by incorporating various moderators, temperatures, and neutron absorbers and then compared, using the thermal peak centerline energy and the general spectrum shape, to determine the likeness of the altered spectrum to the advanced reactor spectrums.

Based on the collected data, the FHR and VHTR core characteristics were best represented with high-temperature, 900 K, graphite in the TRIGA's irradiation location D1. In addition, all

regions of interest where spectrums were found (active core, coolant, graphite, and reflector) can be represented in the same locations. Once the peaks were adequately matched, reactor similarity factors were found which can be used to convert experimental data into predicted FHR or VHTR results in the case of an ensuing experiment.

DEDICATION

I dedicate this thesis to my family: Craig and Susan Marcantel, Grant Marcantel, and Buckeye.

My father, Craig, always pushed me to accomplish my goals because he believed I was capable even when I did not think so.

My mother, Susan, always helped remind me I was human when I forgot.

My brother, Grant, was a comrade and commiserated with me through the peril of graduate schooling. I hope I helped him as much as he helped me.

And finally, my late cat, Buckeye, was always at home to cheer me up after a long, arduous day.

ACKNOWLEDGEMENTS

I would like to thank my committee chair, Dr. Pavel V. Tsvetkov, and my committee members, Dr. Karen V. Kirkland, and Dr. Michael B. Pate for their guidance and support throughout the course of this research.

Specific thanks also go my dear friends Jonathan Scherr and Dr. Carol Gwyn Rosaire for their patience in answering my never-ending questions regarding reactor physics and design; And a special thanks to Jan Vermaak for answering my questions and concerns on behalf of the Nuclear Science Center.

Finally, thanks to the other members of Dr. Tsvetkov's lab and the department faculty and staff for making my time at Texas A&M University a great experience.

CONTRIBUTORS AND FUNDING SOURCES

This thesis is based upon work partially supported by the U.S. Department of Energy under Award Number DE-NE0008306 (IRP-14-7829) and by Texas A&M University.

The work was supervised by a dissertation committee consisting of Professor Pavel Tsvetkov [advisor and committee chair] and Professor Karen Kirkland of the Department of Nuclear Engineering and Professor Michael Pate of Mechanical Engineering. All work for the thesis was completed independently by the student. The initial models for FHR, VHTR, and TRIGA were developed and provided by Prof. Farzad Rahnema of Georgia Institute of Technology, Mathew Johnson and Dr. Thomas Lewis of Texas A&M University, and the Nuclear Science Center, respectively.

Finally, the Fluor Corporation's contribution to the Nuclear Advanced Supply Chain Management Team indirectly attributed towards the financial progression of this work.

NOMENCLATURE

CANDU—Canadian Deuterium Uranium Reactor

FBR—Fast Breeder Reactor

FHR—Fluoride High-Temperature Reactor

FLiBe—Lithium Fluoride, Beryllium Fluoride Salt

HTR—High-Temperature Reactor

INL—Idaho National Laboratory

LWR—Light Water Reactors

MCNP—Monte Carlo N-Particle

MSFR—Molten Salt Fast Reactor

MSR—Molten Salt Reactor

MSRE—Molten Salt Reactor Experiment

ORNL—Oak Ridge National Laboratory

SFR—Sodium Fast Reactor

TAMU—Texas A&M University

TRIGA—Teaching, Research, Isotope, and General Atomics

TRISO—Tristructural isotropic fuel

VHTR—Very High-Temperature Reactor

VISED—Visual Editor (for MCNP)

TABLE OF CONTENTS

LIST OF FIGURES

LIST OF TABLES

INTRODUCTION

Advanced Reactor Designs

There are four generations of reactors. The first generation includes preliminary test "piles" used for proof-of-concept experiments. These are the most basic of reactor designs. Generation II constitutes the majority of the operating nuclear fleet around the world. These were the first reactors designed for power production, and it includes the first Navel reactors, LWR, CANDU, etc. Generations III and IV include the advanced reactor designs. Generation III designs are fundamentally the same as Gen II but with additional inherent safety characteristics. Generation IV includes designs that are on the vanguard of technological and safety advances in reactors. It consists of reactors that were conceptually initiated in the '40-'60s, like the MSR, FBR, and SFR, but it also includes advanced designs of the gen II and III classes. Examples of these would be HTGR/VHTR, MSFR, FHR, etc.

Advanced reactor designs differ from conventional designs in several ways; They operate at higher temperatures to increase thermal efficiency, burn actinides, incorporate hexagonal lattices even in thermal reactors, and utilize advanced manufactured TRISO (tristructural isotopic) fuel particles. In addition, many advanced reactor core designs use a fluoride-lithium, fluoride-beryllium salt (also known as "flibe") as a coolant unlike generation II designs that used light or heavy water. The high operating temperature conditions present material property concerns and extreme thermal stresses for equipment that were not prevalent in the generation II designs. Specifically, water and salts are corrosive especially in higher temperature applications. Because of this and the increased thermal stresses, high operating temperature is a particular challenge of

advanced reactors and the data collection equipment necessary to monitor the reactor's operation. Building an advanced reactor can be risky without proper experimental data to support theoretical claims. For this reason, experiments are completed in currently operating research reactors to represent the environment equipment would see in advanced reactor operating conditions. This can be completed in national laboratory reactors or in university research reactors which are typically more available and cheaper to use. Texas A&M University operates a TRIGA (teaching, research, isotope, and general atomics) research reactor on campus that can be used for such experiments.

Fluoride High-Temperature Reactor (FHR)

FHR Design Overview

The FHR is an advanced, thermal reactor design in the Generation IV class. It is a subset of the MSR group because it utilizes molten salt as a coolant and moderator; however, the FHR has prismatic (solid) fuel unlike the Molten Salt Reactor Experiment (MSRE) at Oak Ridge National Lab (ORNL). This solid fuel can come in the form of fuel pins, fuel plates, or pebbles as is the case with U.C. Berkeley's design. The prismatic fuel structure allows the molten salt to flow between assemblies thus cooling and additionally moderating the core. Because ORNL has maintained prominence in the molten salt reactor industry, it has taken part in the development of the FHR.

There are currently three FHR designs circulating in academia and national labs. The first design includes two variations of solid fuel—fuel pins and fuel plates—both of which are developed either entirely or in part by ORNL. These designs can be seen below in Figure 1. The third design is the Pebble Bed reactor by Berkeley, but it will not be discussed in this research.

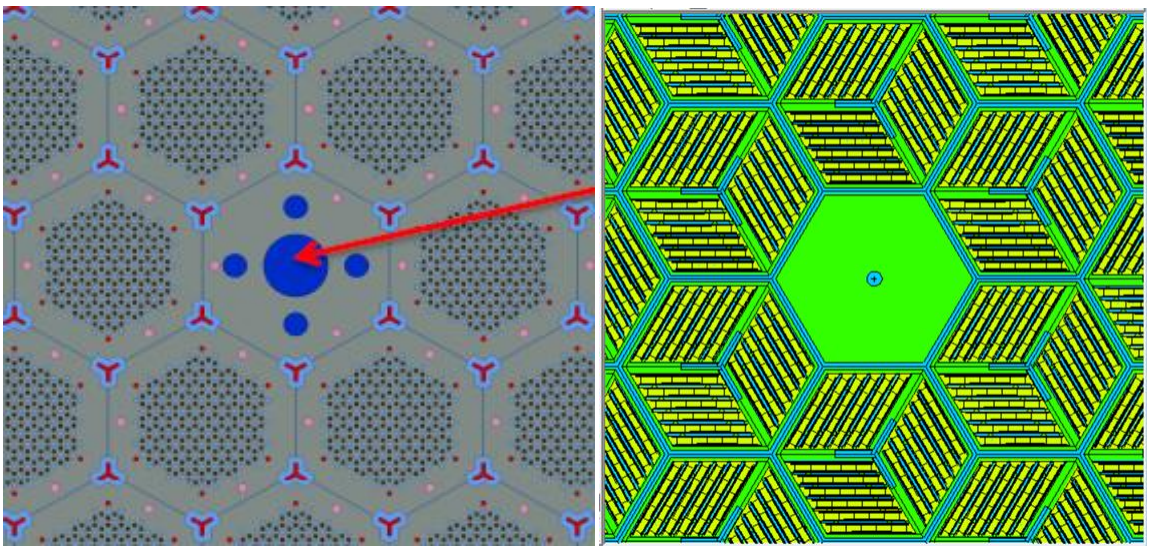

Figure 1: Pin-type fuel FHR design developed in SolidWorks by ORNL and plate-type fuel FHR design developed in MCNP respectively

Plate Type FHR Design

The plate-type design is the focus of this research. The core has a power of 600 MWt and is 5.25 m in diameter. The reactor vessel consists of Alloy 800-H with a 1 cm layer of boron between the core and the vessel as shown in Figure 2. There are 252 hexagonal fuel assemblies in the active core region, and the core is surrounded by graphite reflector blocks.

Each fuel assembly is 45 cm from one flat end to the opposite. The Y-shaped center in the assembly of Figure 2 represents the control rod slot which is filled with flibe represented in blue. Each fuel assembly has one central control rod. The yellow sections represent graphite at 1200 K with semi-circle spacers to allow coolant flow. The black strips represent compact TRISO fuel

particles enriched to 9 wt% uranium-235 (^{235}U) in accordance with the MCNP file. The central matrix consists of graphite which also moderates neutrons. In addition, small Eu_2O_3 (^{151}Eu and ^{153}Eu) spheres are in the graphite matrix to act as burnable absorbers, but these are not visible in the given figures (FHR Model).

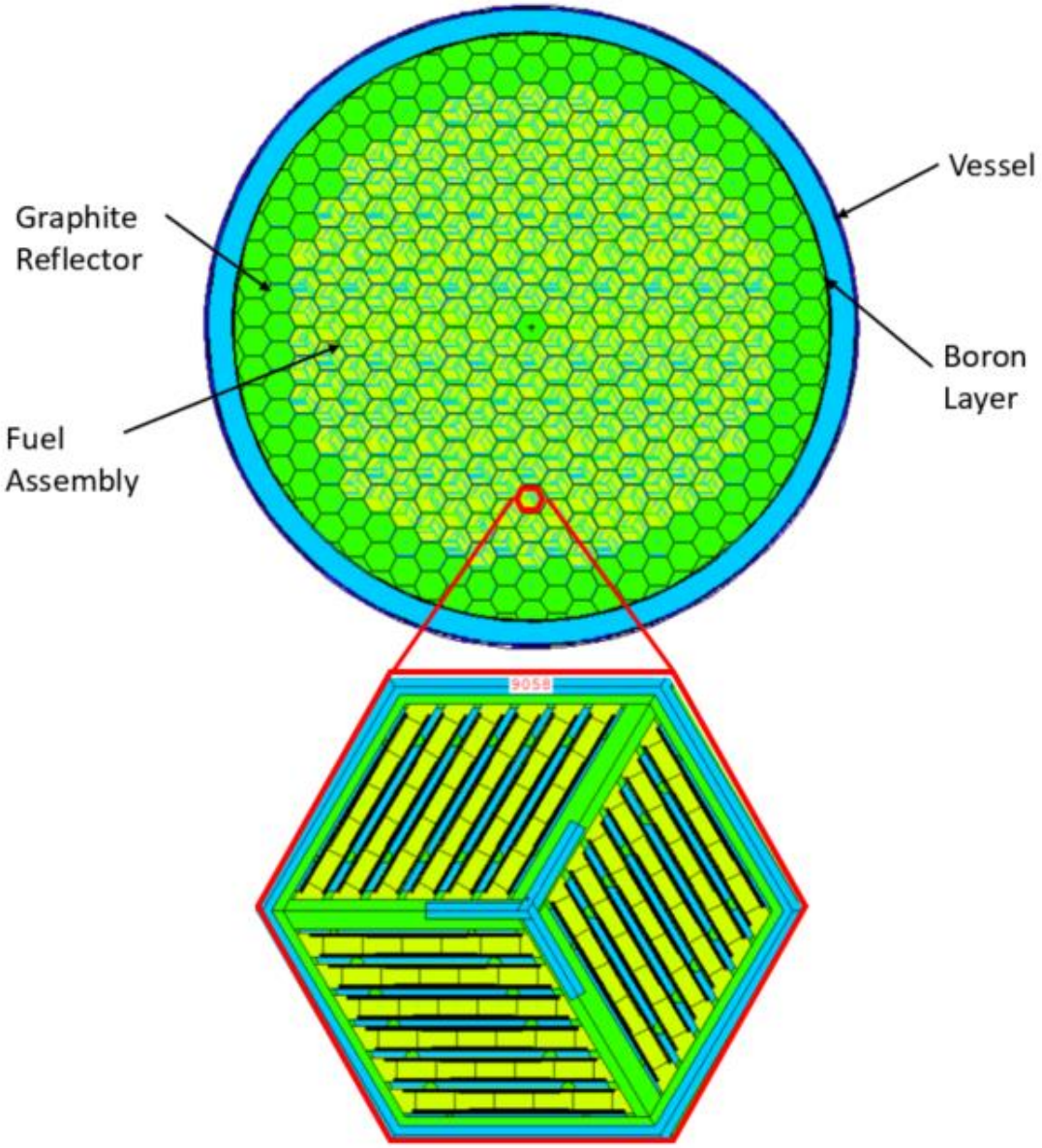

Figure 2: Detailed VISED picture of active core and zoomed-in fuel assembly

FHR Fuel and Neutronics

FHRs and MSRs were designed for commercial power production, so all designs require <20% ^{235}U enrichment; However the MSR can operate using either the uranium fuel cycle or the thorium fuel cycle, but a "driver" material is required to maintain the neutron population needed to breed ^{233}U out of ^{232}Th. This is because ^{232}Th is a fertile material—not a fissile one [1].

Table 1: FHR design characteristics

Parameter	FHR
Power (MWth)	600
Pressure (atm)	1
Fuel Temperature (K)	1200
Lattice	Hexagonal
Thermal Flux Peak Energy (MeV)	1.91E-07
Thermal Flux Peak (n/cm2*s)	6.79127E+11
Moderator	Graphite
Coolant	Flibe
Fuel	UO_2
Fuel Design	TRISO
Enrichment (wt %)	9
Core diam. / Active Core diam. (m)	10.5 / 9.6
Core height / Active Core height (m)	19.5 / 5.5
Number of fuel assemblies	252
Burnable Absorber	Eu-203
Control Rod Material	Mo and Hf

Thermal reactors have softer spectrums meaning they have lower energy neutrons on average. This makes them more sensitive to fission product buildup, so fission product removal is of great importance. Softer energy spectrums do not burn away higher z materials and actinides because the neutrons are not energetic enough to induce fission. The FHR's higher operating temperature results in higher energy neutrons which can burn actinides. This is one of the reasons why this design is particularly desired. Details of the FHR's design and operating characteristics can be seen in Table 1.

FHR Coolant Salt

Advanced reactor salts are either fluoride-based or chloride-based salts depending on whether the spectrum is soft or hard respectively. Both salts are chemically inert with air and water unlike the sodium used in other reactor designs [5]. In traditional MSR designs, the fuel is dissolved in a carrier salt which then acts as both fuel and coolant. The salts are typically a binary or a ternary carrier salt with a single or binary fuel salt. The two main salts are then mixed to form the final salt mixture. "Flibe" is the colloquial name for a commonly used eutectic salt (LiF-BeF-UF_4) used in advanced designs. The FHR design utilizes flibe only as a coolant—the salt does not contain fuel.

Fluoride-based salts are typically used due to its tendency to thermalize neutrons in thermal reactors. This aids to thermalization thus decreasing the amount of moderator (typically graphite) required to bring the core to a critical state. Alternatively, chloride salts are better contestants for molten salt fast reactors. The inelastic scattering microscopic cross sections can be seen in Figure 3 [2]. As shown, ^{19}F does tend to interact and slow down neutrons until about 100 keV. Chlorine,

both ^{35}Cl and ^{37}Cl which make up 25% and 75% of natural chlorine respectively, do not interact with neutrons at energies below 1.25 MeV [3]. This means that chlorine does not continuously slow down neutrons into the thermal range; however, chlorine and fluorine salts will thermalize neutrons thus giving all MSR designs softer spectrums than other fast reactor designs.

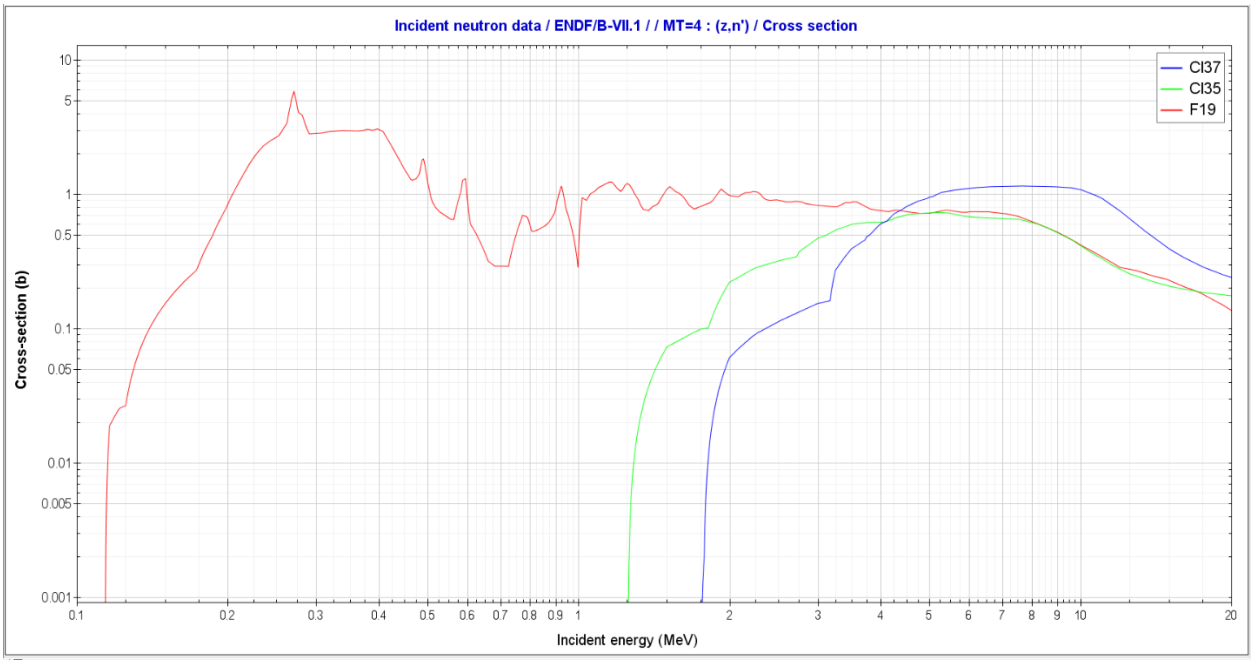

Figure 3: Inelastic scattering cross sections for fluorine and chlorine

Very High-Temperature Reactors (VHTR)

VHTR Design Overview

High-temperature reactors (HTR) operate at significantly higher temperatures in comparison to traditional generation II light water reactors (LWR). These reactors operate in the ranges of 650°C to 1000°C, where LWRs operate around 300°C to 350°C [4]. These HTRs are of interest to the power industry for a few reasons. Firstly, the higher temperatures allow for higher power conversion efficiencies. This is obviously of interest because it reduces the cost of energy per kilowatt hour. The second is the reactor's excessively high waste heat can be used in hydrogen production for other industries. Lastly, the higher temperatures burn actinide fission products as mentioned in previous sections. For these reasons, high-temperature reactors are of interest to the power industry and are thus a topic of research in the modern era.

The VHTR is a uranium fueled, graphite moderated, and helium cooled design proposed in the HTR umbrella group. The particular version of interest for the purpose of this research is the VHTR designed and proposed by General Atomics. A top-down view of the VHTR schematic core design can be seen in Figure 4.

The active core has ten axial sections which are each 79.3 cm tall, and the effective core radius is 304.9 cm. The core consists of three main sections: the inner graphite reflector, fuel ring region, and the outer graphite reflector. The particular design that will be analyzed for this research is the 600 MWt design. Additional features of the reactor can be seen in Table 2 [5].

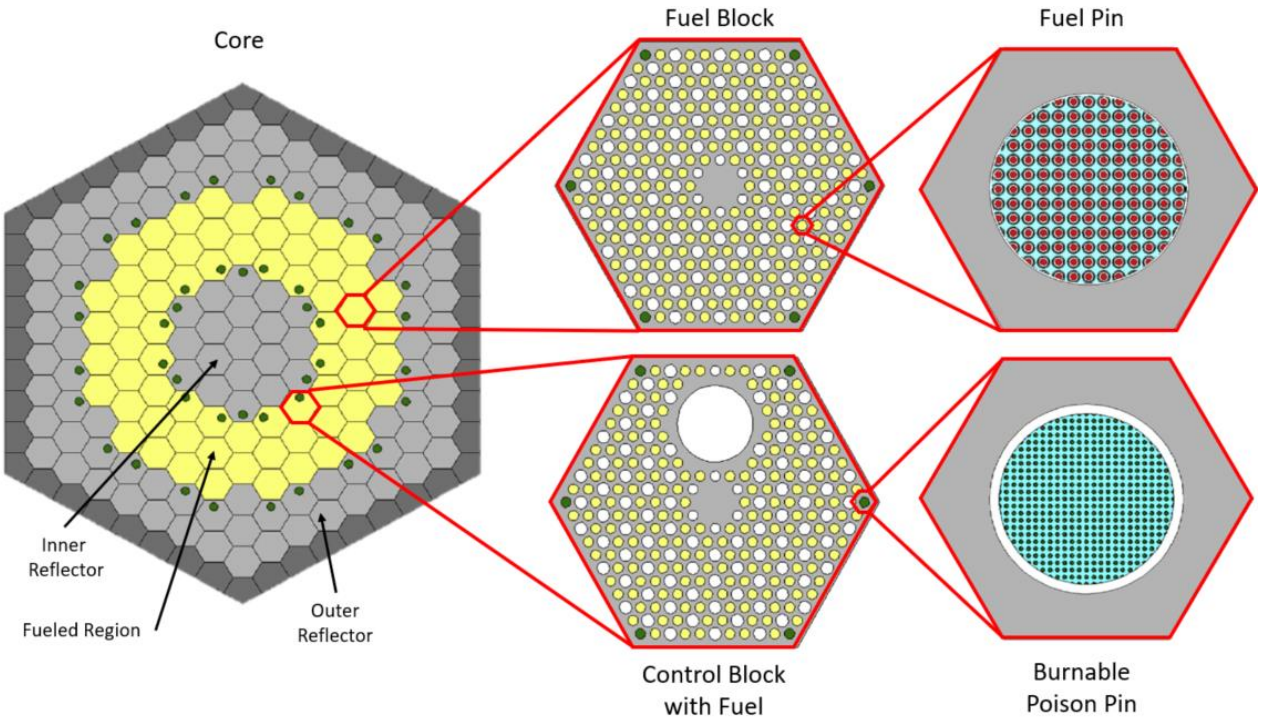

Figure 4: Very high-temperature reactor prismatic core schematic with zoomed in fuel block, control block, fuel pin, and burnable absorber pin

Table 2: VHTR operating parameters (600 MWth version)

Parameter	VHTR
Power (MWth)	600
Pressure (atm)	1
Fuel Temperature (K)	1200
Lattice	Hexagonal
Thermal Flux Peak Energy (MeV)	2.53E-07
Thermal Flux Peak (n/cm^2*s)	1.3457E+13
Moderator	Graphite
Coolant	Helium
Fuel	UO_2
Fuel Design	TRISO
Enrichment (wt %)	15.5
Core diameter (m)	6.1
Core height (m)	10.7
Number of fuel assemblies	66
Control Rod Material	Boron
Average Power Density (W/cc)	6.5
Inlet Temp (°C)	490
Coolant Flow Direction	Downward
Core Geometry	Annular
Inner Reflector Eff. Radius (m)	1.48
Active Core Eff. Radius (m)	2.41
Outer Reflector Eff. Radius (m)	3.33
Number of Fuel Columns	102
Number of Fuel Blocks per column	10 (600 MWt version)
Active Core Volume (m^3)	90.767 (600 MWt version)
Active Core Height (m)	7.93 (600 MWt version)
Fuel Element Geometry	Fort St. Vrain
Fuel Particle(s)	Fissile only

VHTR Fuel and Neutronics

The fuel utilizes TRISO fuel particles with an effective enrichment 15.5 wt%. The VHTR is similar to the FHR in that both cores have hard, thermal spectrums. This means that while the fission chain reaction is maintained via thermal neutrons, the energies of said neutrons are higher than the generation II LWR designs. In addition, the VHTR and FHR both have graphite as the main moderator in the core; therefore, the neutron spectrums of both reactors have common characteristics.

Teaching, Research, Isotopes, and General Atomics Reactor (TRIGA)

TRIGA Design Overview

Texas A&M University has a TRIGA reactor that is used for educational purposes, graduate student research, and external industry contracts. This design, a TRIGA Mark II, is a thermal, pool-type design rated at 1 MWt. The light water is both the coolant and moderator in this reactor design.

This reactor design has several in-core irradiation locations, D3 and D7, that can be seen in the following Figure 5. These locations are where experiments can take place inside of the core. In addition, there are outer reflectors that can be removed for the purpose of experimental setups. These are shown by all variations of green in Figure 5.

Fuel and Neutronics

The prismatic fuel pins, which are shown by white circles in Figure 5, are <20% enriched with ^{235}U, and the light water coolant/moderator is shown in blue. The TRIGA's neutron flux

ranges from 1E12 n/cm^2*s to 1.4E13 n/cm^2*s [6] with the peak in the D3 location of 3.93E11n/cm^2*s. The thermal neutronics nature of the TRIGA reactor and its ability to be altered for experimental setups easily and safely makes it a viable option to further the development of the FHR and VHTR designs.

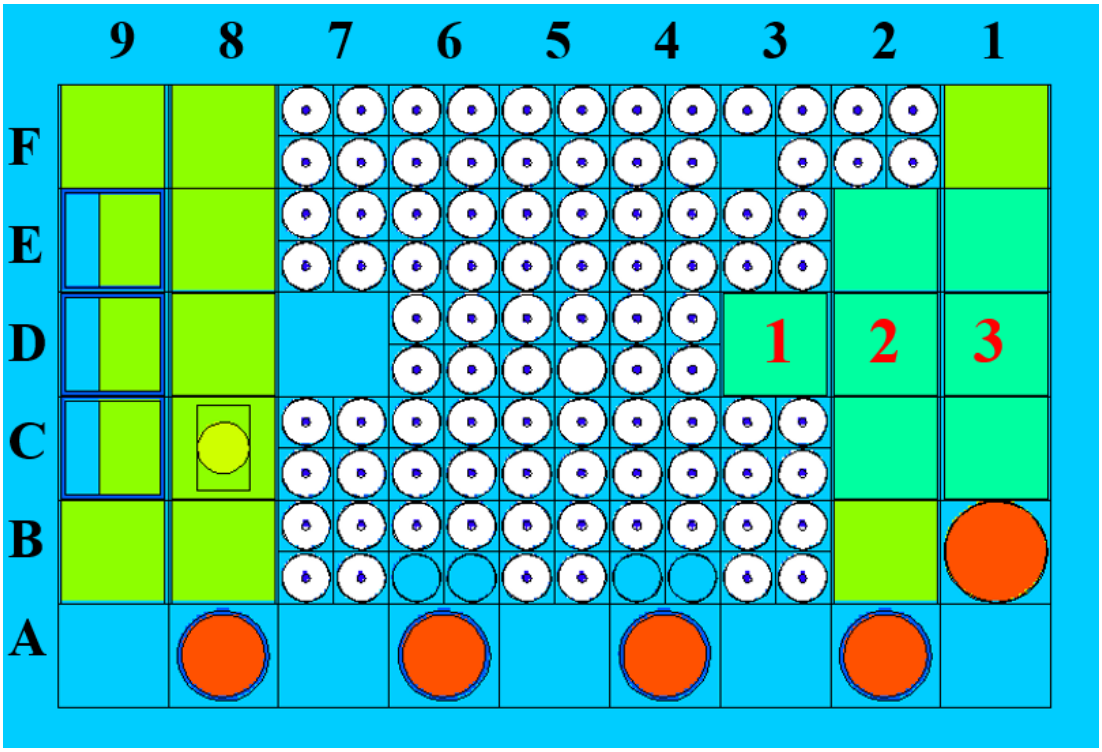

Figure 5: Simplified TAMU TRIGA diagram with rod positions and grid positions

Reactor Comparisons

These three reactors are drastically different in design, but they share similar operating characteristics, such as similar operating pressures and transparent coolants, that allow for data comparison. Some of these characteristics are shown in Table 3.

The FHR and VHTR active core region energy spectrums can be seen in Figure 6 along with the energy spectrum obtained from the in-core irradiation location, D3, in the TRIGA. The FHR and VHTR energy spectrums have relatively similar shapes as shown in the thermal and epithermal regions below ~ 1E-2 MeV, but the TRIGA's spectrum is significantly different. The VHTR at full power (600 MWt) yielded high thermal neutron fluxes thus dwarfing the peaks of the FHR and TRIGA spectrums. For easier visual comparison, the VHTR power level was reduced to 10 MWt in the graphs throughout the rest of this report unless otherwise noted.

Table 3: Reactor operating characteristics of FHR, VHTR, and TRIGA

Parameter	FHR	VHTR	TRIGA
Power (MWt)	600	600	1
Pressure (atm)	1	1	1
Fuel Temperature (K)	1200	1200	600
Lattice	Hexagonal	Hexagonal	Square
Thermal Flux Peak Energy (MeV)	1.91E-7	2.53E-7	5.06E-8
Thermal Flux Peak (n/cm^2*s)	6.79E11	1.35E13	3.93E11
Moderator	Graphite	Graphite	Light Water
Coolant	Flibe	Helium	Light Water
Fuel	UO_2	UO_2	U-ZrH
Fuel Design	TRISO	TRISO	pin
Enrichment (wt %)	9	15.5	<20

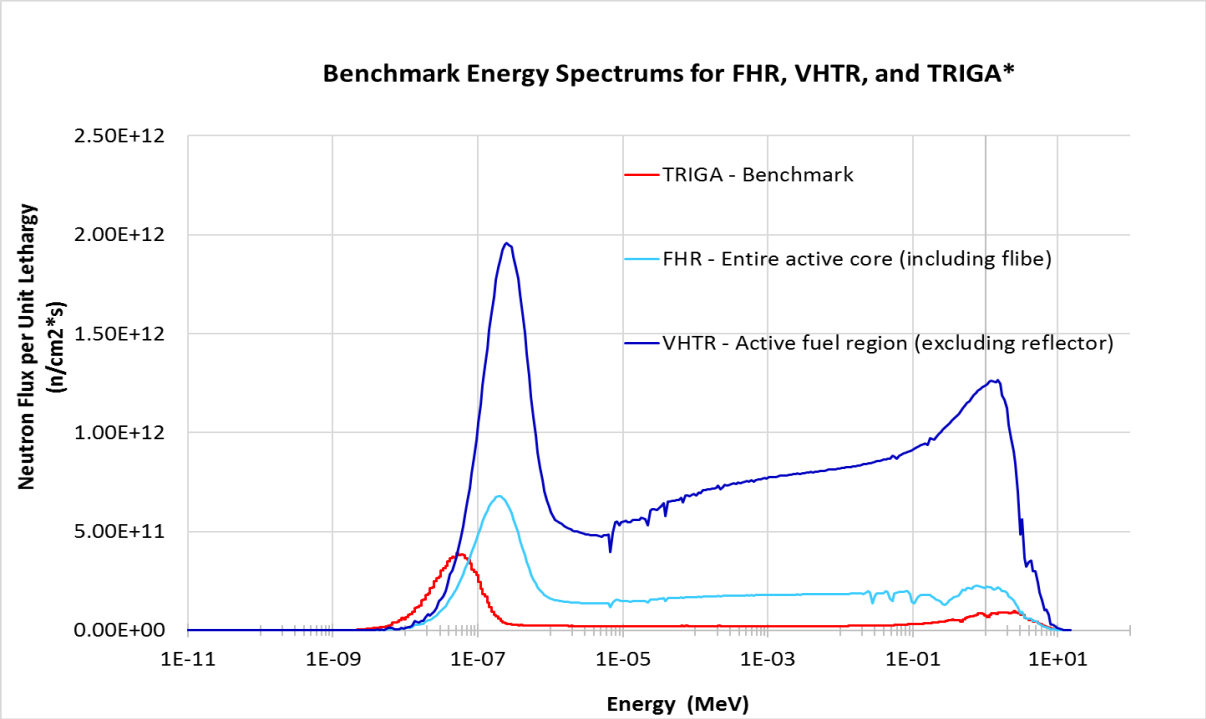

*VHTR at 600 MWt (100% power)

Figure 6: Benchmark energy spectrums of all three reactors: TRIGA, FHR, and VHTR

OBJECTIVES

The purpose of this research is to emulate advanced reactor operation conditions using TAMU's TRIGA reactor. This will facilitate further R&D efforts and expand available experimental capabilities for advanced reactor development efforts. Though no experiment is planned to follow this research, the results would assist in converting experimental results obtained in TAMU's TRIGA reactor to data that would be obtained in a true FHR or VHTR demonstration reactor if an experiment were developed. To determine similar factors between reactor designs, a Monte Carlo N-Particle (MCNP) code will be used to tally relevant reactor physics characteristics in each reactor design. In turn, this will aid in advancing the development and construction of the FHR and/or VHTR demonstration reactors and provide a method of comparison that can be used between the TRIGA reactor and other advanced reactor designs. This is important for future generation reactors because the designs must be validated first through experiments conducted in other reactors. One of the main reasons for these experiments is to determine how the core's advanced equipment will maintain integrity in high radiation and high temperature environments.

In the case of an experiment, the existing reactor (TRIGA) will require modifications to represent the reactors of interest (FHR and VHTR). This means altering the neutron flux inside a particular in-core location to represent the neutronic and general operating conditions that would be seen in an advanced demonstration reactor.

These experiments can take place only in already operating reactors, so there are two options: national laboratory research reactors and university research reactors. National lab reactors will be significantly more expensive but are not necessary for many irradiation

experiments. There are several reasons why the TAMU TRIGA reactor is adequate for the intended research into advanced reactors. As mentioned before, the TRIGA reactor is a thermal, pool type design rated at 1 MWt with light water as both the coolant and moderator. This is similar to both the FHR and VHTR designs which are thermal reactors and have transparent coolants as well. This results in similarly shaped neutron energy spectrums as shown in Figure 6. In addition, these experiments could include not only irradiation experiments but also optical experiments due to the similarities in the coolant/moderator. Finally, the TRIGA reactor has similar pressure and fuel to the other reactors which are presented in Table 3. This makes the TRIGA reactor a reasonable and cheaper alternative to using a national lab research reactor. In addition, for the development and testing of advanced reactor equipment, a high neutron environment is not required. The focus of advanced equipment testing is concerned with the overall response and adequacy of the equipment in the operating conditions. This means proving the equipment can operate in a neutron radiation environment in general. Because the TRIGA reactor's flux is significantly lower than other reactor fluxes, specific irradiation fluence experiments may be better completed in specialized high irradiation reactors.

There are some drawbacks to utilizing the TRIGA reactor. Firstly, the spectrums do not match exactly, so the TRIGA reactor irradiation locations need altered neutronics to correctly represent the effects that would be seen in the FHR and VHTR. Secondly, the TRIGA reactor has a lower neutron flux than other national lab reactors, so experiments will require longer run times to acquire the same neutron fluence. Even so, these two drawbacks would arise independent of the research reactor design, and they are not significant enough to rule out the usage of a TRIGA reactor for preliminary experiments to further the FHR and VHTR designs.

REACTOR PHYSICS SIMILARITY FACTORS

To convert true experimental results to theoretical advanced reactor predicted results, reactor similarity factors must be obtained to convert the data. The similarity factors ultimately represent a multiplying number that can convert experimental data to represent advanced reactor data. For this reason, the similarity factors between reactor designs are focused on the neutron flux and total neutron fluence which are represented by Eq. (1) and Eq. (2) respectively.

$$\phi(\vec{r}, t) = v \cdot N(\vec{r}, t) \tag{1}$$

$$\Phi(\vec{r}, T) \equiv \int_0^T \phi(\vec{r}, t)\, dt \cong \phi(\vec{r}) \cdot T \tag{2}$$

N=atom density (atoms/cm^3)
v=neutrons per fission source

To calculate this similarity factor, the neutron spectrums of the FHR and VHTR regions of interest will be divided by the TRIGA data. This will result in a multiplication factor that, once multiplied by the experimental output, will cancel the TRIGA data leaving FHR or VHTR predicted results. These neutron energy spectrums can be collected by tallying the neutrons in MCNP. This will find the distribution of neutrons in given energy bins. Using the tallied information from the TRIGA, FHR, and VHTR models, similarity (conversion) factors between flux tallies can be calculated.

APPLIED CODES

There are two types of transport codes in the nuclear realm: deterministic and Monte Carlo. Deterministic codes utilize the neutron transport equation along with other mathematical relations to calculate results. This type of code is computationally inexpensive, but many assumptions must be made, and complex geometries are laborious if not impossible. In addition, the results are only as good as the inputs and assumptions. On the other hand, Monte Carlo codes do not calculate results based on mathematical relationships; It develops a list of pseudorandom numbers, and each number represents a particle. These particles run throughout the simulation geometry and are tracked until they are either absorbed or escape. These particles move throughout the geometry where interactions are dependent on the probability of a collision within a given material. Because the interactions of particles and materials is based on probability, assumptions to the system are not required as an input; The required inputs are geometry, materials, and a particle source. These codes are computationally expensive because they track each particle, but they are advantageous because complex, 3-dimentional geometries can be developed.

MCNP has many abilities, and this research focuses on criticality calculations, tallying of neutron fluxes, and extended burn calculations. Criticality calculations determine the k_{eff} of the given geometry and materials of any 3D design. Tracking each particle allows MCNP to count (tally) particles of interest as they pass through a given surface or body of the 3D model. There are several types of tallies that can be taken, and they are shown in Table 4 [7].

Table 4: Various tally indicators, physical quantity, and units that can be taken using MCNP6 software

Tally	Physical Quantity	Units
F1	$J = \int dE \int dt \int dA \int d\Omega \left\lvert \hat{\Omega} \cdot \hat{n} \right\rvert \Psi(\vec{r}' \cdot i, \bar{t} \cdot t)$	particles
F2	$\bar{\phi}_s = \frac{1}{A} \int dE \int dt \int dA \int d\Omega \, \Psi(\vec{r}, \hat{\Omega}, E, t)$	particles·cm^{-2}
F4	$\bar{\phi}_v = \frac{1}{v} \int dE \int dt \int dA \int d\Omega \, \Psi(\vec{r}, \hat{\Omega}, E, t)$	particles·cm^{-2}
F5	$\phi_P = \int dE \int dt \int d\Omega \, \psi(\vec{r}_p, \hat{\Omega}, E, t)$	particles·cm^{-2}
F6	$H_t = \frac{\rho_a}{m} \int dE \int dt \int dV \int d\Omega \, \sigma_t(E) H(E) 4(\vec{r}, \hat{\Omega}, E, t)$	MeV·g^{-1}
F7	$H_f = \frac{\rho_a}{m} Q \int dE \int dt \int d\Omega \, \sigma_f(E) \psi(\vec{r}, \hat{\Omega}, E, t)$	MeV·g^{-1}
F8	pulses	pulses

For this research, the F4 tally was used to determine the flux in each volume of interest. This is an important metric considering the neutron characteristics of the reactor must be known in the case of experimental comparison. The data collected by advanced equipment must be compared to the collected data retrieved using MCNP. MCNP collects this information by tracking particles moving through a given cell geometry per source particle. The MCNP output units are particles/cm^2*source [8]. These are not the proper units of flux, so the data must be adjusted to

account for the type of fissile fuel being used and the thermal power of the reactor. This is done using Eq. 3 with the units displayed below in Eq. 4 [8].

$$\boldsymbol{\phi = (MCNP)\left(\frac{1}{V}\right)\nu(1E6)P(3.12E10)} \quad \textbf{(3)}$$

$$\boldsymbol{\phi = \frac{n * cm}{cm^2 * s} = \frac{n}{cm^2 * s} = \left(\frac{n * cm}{souce}\right)\left(\frac{1}{cm^3}\right)\left(\frac{source}{fission}\right)\left(\frac{1E6\,W}{MW}\right)(MW)\left(\frac{3.12E10\ fission}{W * s}\right)} \quad \textbf{(4)}$$

1st term—MCNP output
2nd term—inverse volume
3rd term—average number of neutrons given off in one fission event (2.4 for U-235)
4th term—conversion factor from Watts to megawatts
5th term—Reactor thermal power
6th term—Conversion factor from fission energy to Joules
(calculation of neutron flux characteristics of using MCNP4A code).

After combining the constants and ν=2.4 source particles/fission, the constant multiplier for a uranium fueled reactor is 7.488E16 source/MW*s. These units do not mean anything useful, but the product of this constant, reactor power, and the MCNP output results in correct flux units. MCNP automatically calculates the volume of the indicated cell, but it does not always do this correctly especially when complex geometries are present. To circumvent this issue, the correct volume, calculated by the user, can be placed in the SD callout below the tally callout. This indicates by what volume the tally is to be divided. Finally, the thermal output of the reactor is needed to correctly determine the flux.

TRIGA MCNP Model Description

The TRIGA core, pool, and building are all modeled in Figure 7, and a more detailed view of the core is shown in Figure 8. In Figure 8, the fuel rods, graphite blocks, and water is shown by the colors white, green, and blue respectively. In addition, the light green rods in the core represent the control bundles, and the in-core irradiation location D3 is labeled. This location is where the majority of the TRIGA tallies were taken because it is where experiments can be inserted into the core with relative ease.

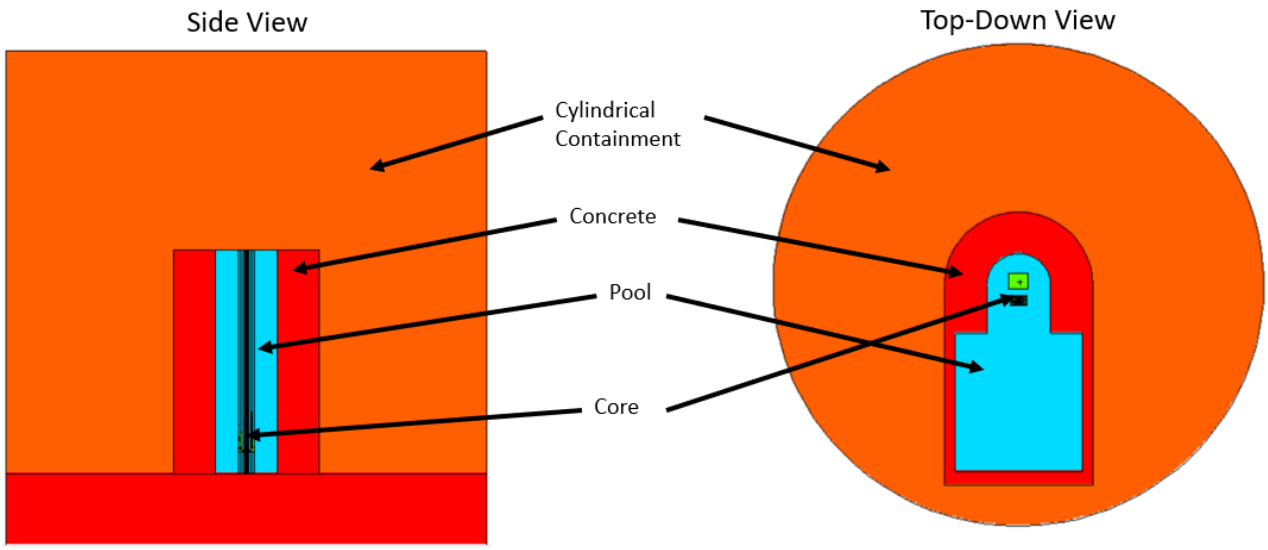

Figure 7: TRIGA model overview including containment building, pool, and reactor core

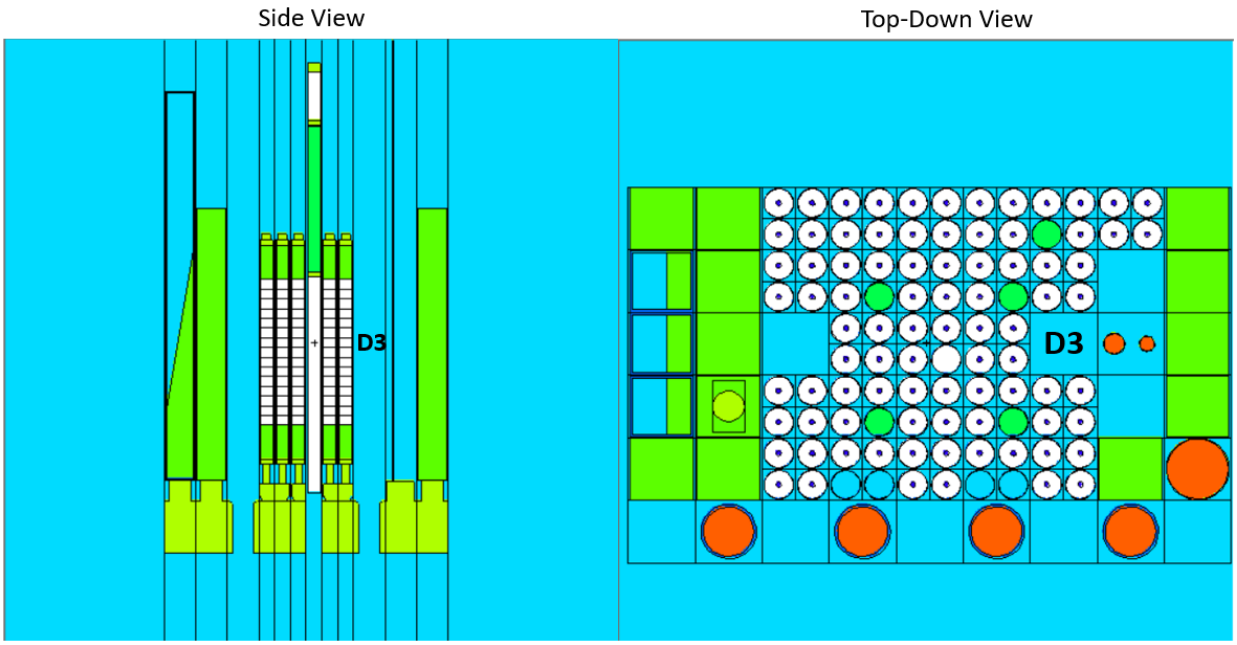

Figure 8: Side and top-down views of TRIGA core

FHR MCNP Model Description

The FHR model includes the entire active core region and the surrounding reactor vessel. Details of the FHR model are shown in Figure 2 and Figure 9. A detailed top-down view of the active core region is in Figure 2 with a detailed view of a single fuel assembly. The green and yellow both represent graphite but at various temperatures. The green graphite is at 900 K, and the yellow represents 1200 K indicated by 6000.72c and 6000.73c respectively in the code. Figure 9 shows a side view of the entire vessel and the corresponding axial cross sections with the active

core region labeled. The light blue color represents the flibe that flows throughout the core, and the red lines, directed along the core's y-axis, are the control rods. These rods are in a fixed position; therefore, all data collected from the FHR model can be represented only in the fully withdrawn configuration of the control rods.

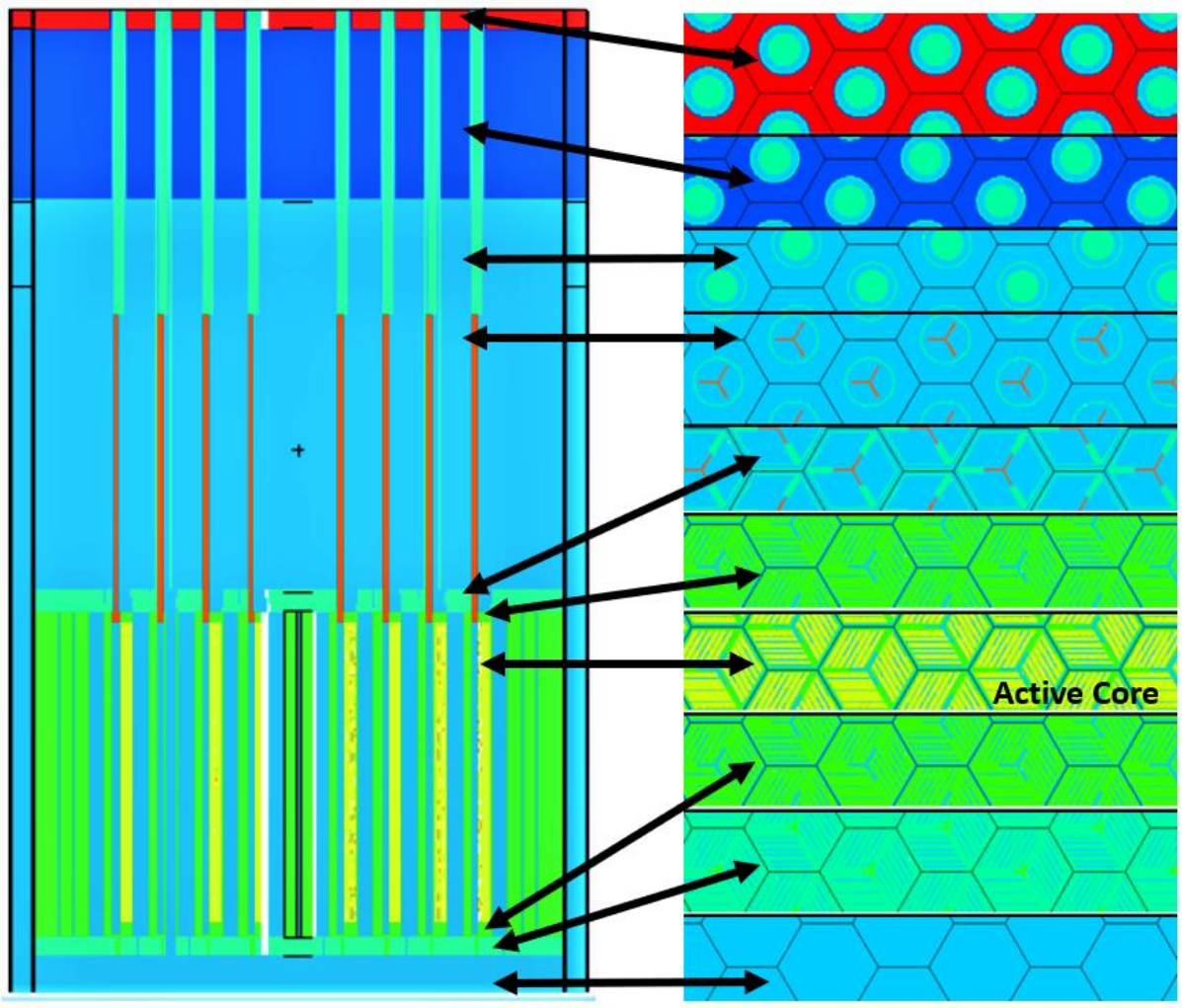

Figure 9: FHR model side view and corresponding axial cross sections

VHTR MCNP Model Description

The VHTR MCNP model is shown in Figure 10. It is important to notice various similarities and difference from Figure 4. Figure 10 shows the inner reflector, fueled region, and the outer reflector, but the shape of the total core in the MCNP model is circular as opposed to the hexagonal shape of Figure 4. For the research presented in this report, the MCNP model is the actual design used to collect results. The colors represent different materials in the figure: yellow represents the helium coolant, multi-color regions in the fuel assembly represent the fuel, and orange represents graphite. Finally, a side view of the VHTR model is shown in Figure 11. A criticality code was run on the VHTR model, and it has a k_{eff} of 1.40047 with a 1σ (standard deviation) of 0.00178.

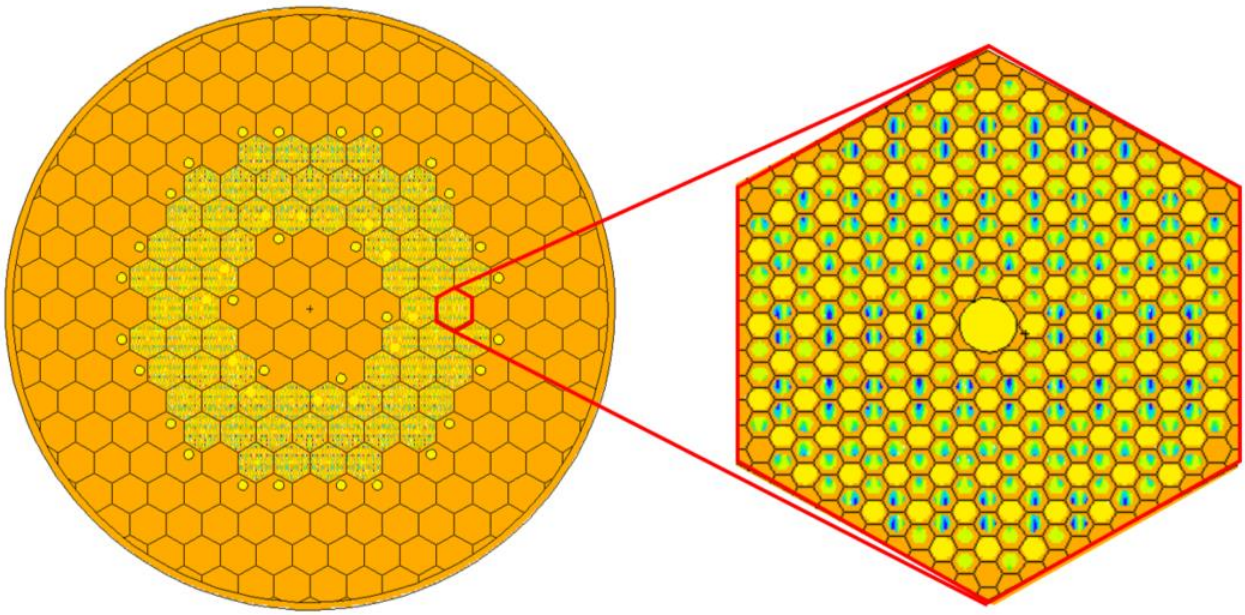

Figure 10: Top-Down view of VHTR MCNP model of core with zoomed in fuel block

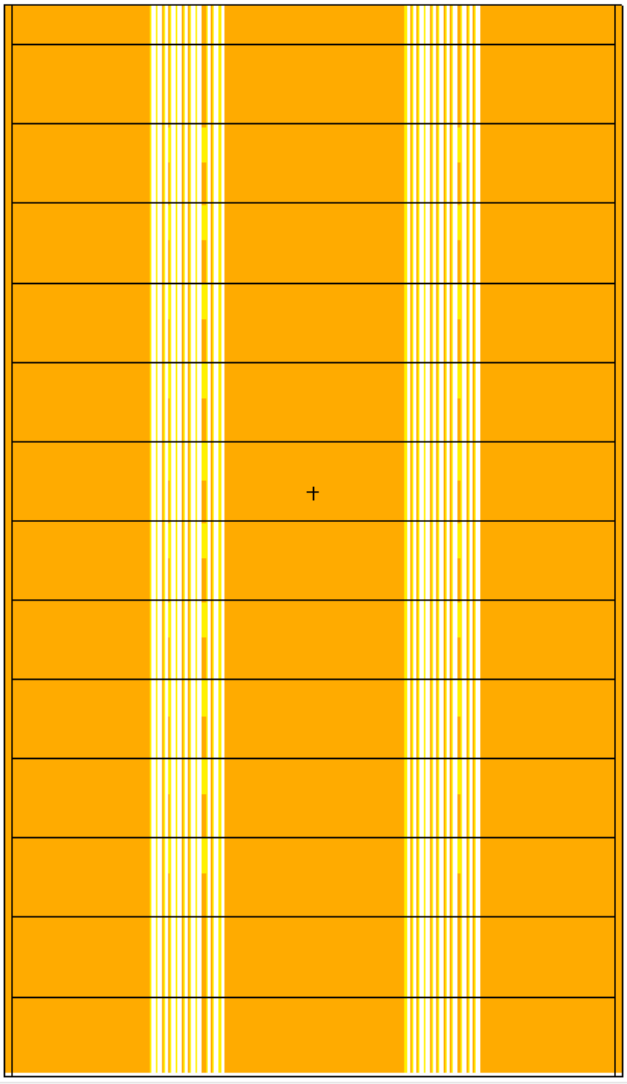

Figure 11: Side view of VHTR MCNP model

SIMULATION APPROACH

The FHR input required a source tape file to run, but this file was never received. To circumvent this, a 0.5E-5 cm diameter fuel bead was placed in the center of the reactor. With knowledge of the fuel bead's location, a point source was used in the initial kcode run. According to the output, the FHR design was confirmed to have a k_{eff} of 1.07251 ± 0.00094. Alternatively, the TRIGA and VHTR models were run without alterations, and each yielded a k_{eff} of 0.99784 ± 0.00051 and 1.40047 ± 0.00178 respectively. These models are assumed complete, critical configurations.

This research will aid in determining how advanced equipment will resist strenuous operating characteristics, such as neutron radiation damage and temperature, in an FHR and VHTR demonstration reactor core. For this reason, the active core neutron energy spectrum is of interest, and an F4 tally was collected over pertinent in-core areas such as the active core, coolant, and moderators. As for the TRIGA, only in-core irradiation locations are of importance because these are where experiments would take place. D3 was chosen as the location of interest because it is one of these irradiation locations; therefore, the energy spectrum of D3 was found and used as comparative data. The D3 location was originally incorporated into the pool of the reactor. However, only the in-core portion of D3 was of interest, so a cell was developed to enclose the in-core position. Therefore, collecting a tally over just the in-core cell could be found. This cell is

shown and labeled in Figure 12, and its volume is 0.00413 m^3 (4129.54 cm^3). As for power, the FHR flux magnitudes are based on a 600 MWt demonstration reactor, and the TRIGA flux is based on the nominal operating power of 1 MWt. Using these values and the conversations of Eq. 3 and Eq 4., the FHR, VHTR, and TRIGA spectrums are shown in Figure 6 (mentioned previously).

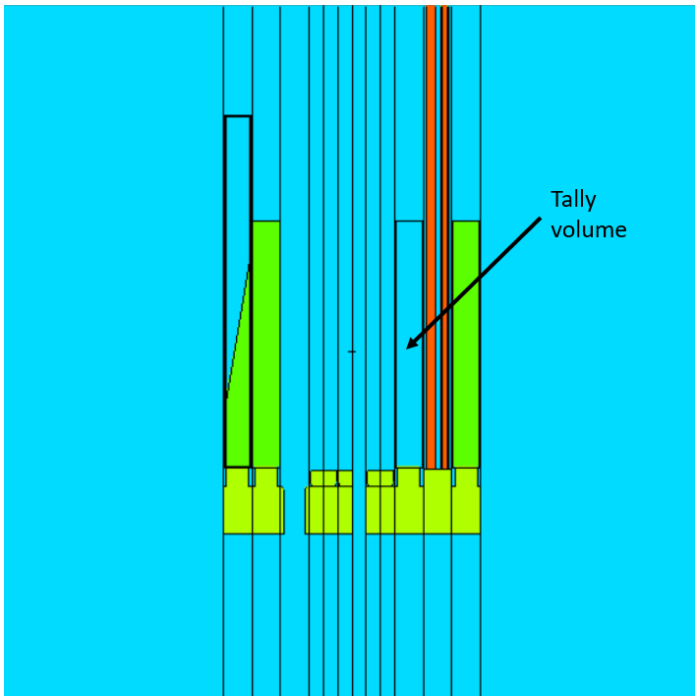

Figure 12: Side view of TRIGA core indicating tally cell volume

As mentioned before, the FHR and VHTR utilize graphite as the main moderator, so similarities between the energy spectrum shapes can be seen in Figure 6. The FHR and VHTR benchmark data was collected over the active core region including the coolant. The flibe in the FHR also moderates neutrons which accounts for some of the difference between the FHR and

VHTR spectrum shapes. In addition, the FHR has a lower fast spectrum peak due to the increased thermalization of neutrons. Finally, the peaks of both the FHR and VHTR have significantly higher energy averages in the thermal peak region. The energy peaks of the FHR, VHTR, and TRIGA reactors are 1.91E-7 MeV, 2.53E-7 MeV, and 5.06E-8 respectively.

As Figure 6 depicts, the FHR and VHTR energy spectrums are significantly harder than the TRIGA spectrum. The thermal peaks will need to be comparatively similar to get accurate data out of experiments. This is where the basis of this research is situated: altering the TRIGA spectrum to better match the FHR and VHTR spectrums.

REACTOR PHYSICS ANALYSIS AND METRICS DEVELOPMENT

Cases and Approach

To alter the neutronics of the TRIGA reactor to better represent the FHR and VHTR, theoretically possible and physically possible situations must both be considered. The theoretically best-comparison results may be impossible to implement physically in a TRIGA experimental setup. For this reason, some of the researched cases will produce the best-comparison results, and others will not have optimal results but are physically realizable.

Several factors can change neutronics. Some of the few are utilizing different moderators, varying the temperature of materials, introducing neutron absorbers and chemical shims, and finally, changing the tally location in the core will yield different spectrums. These factors were altered, results analyzed, and best-comparison and physically realizable determinations made. Details are presented in the following sections. Once the best cases were determined, the reactor similarity factors (ratio of fluxes) will determine the likenesses between the FHR and TRIGA spectrums and the VHTR and TRIGA spectrums. Finally, a depletion calculation was completed on the TRIGA core to determine whether time would be a limiting factor on any experiment. If the core can maintain FHR and VHTR spectrum likeness indefinitely, then no experiment will be limited by time.

RESULTS, ANALYSIS, AND DISCUSSION

Since experiments are to represent in-core operating conditions of the FHR and VHTR, the TRIGA core was altered in the D3 location. The first half of the results will show the comparison between the TRIGA and the FHR followed by the TRIGA and VHTR comparison. Various locations in the FHR and the VHTR were tallied so experiments can represent conditions seen at various points in the core. This required various energy spectrums of FHR and VHTR locations to be found instead of a general, all-encompassing reactor core energy spectrum.

General shape and thermal peak energy similarities between the TRIGA, FHR, and VHTR spectrums is desired. For this reason, the goal is to shift the TRIGA's thermal peak to match the FHR and VHTR thermal peaks. This is accomplished by comparing the energies at which the thermal peaks are centered (henceforth referred to as the "centerline energy").

TRIGA and FHR Comparison

Figure 13 and Figure 14 show the energy spectrums of FHR locations of interest in comparison to the TRIGA benchmark data. As shown, all FHR energy spectrums will be compared separately since the centerline energies are different; However, both reflectors center over the same energy and thus will be considered as one. This is shown in Table 5 along with additional energy data.

Both reflector thermal peaks center on 1.78E-7 MeV, and the fluxes in the reflectors are low in comparison to the TRIGA data; Therefore, Figure 14 is a log-log graph unlike the log-lin of all other graphs. The replaceable reflectors peak is high enough to visually see in a log-lin graph, so it will be representing both the spectrum of the replaceable and permanent reflectors in future graphs.

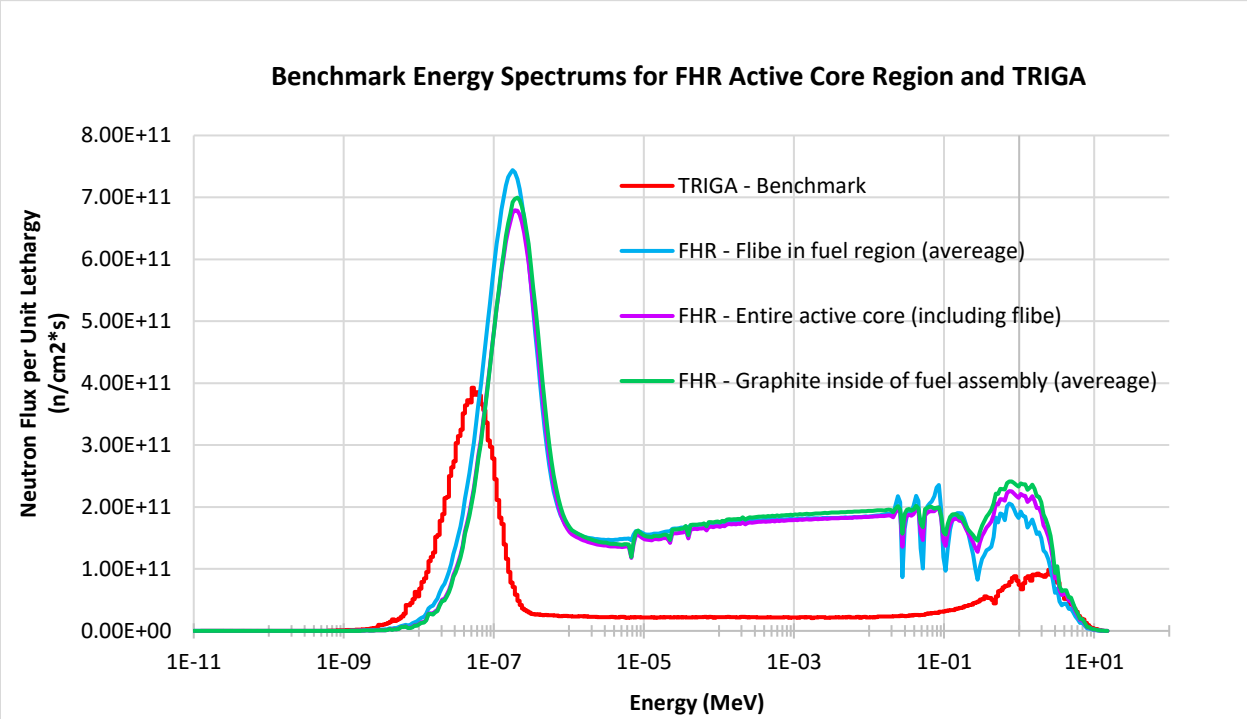

Figure 13: Benchmark energy spectrums for the FHR active core region and TRIGA

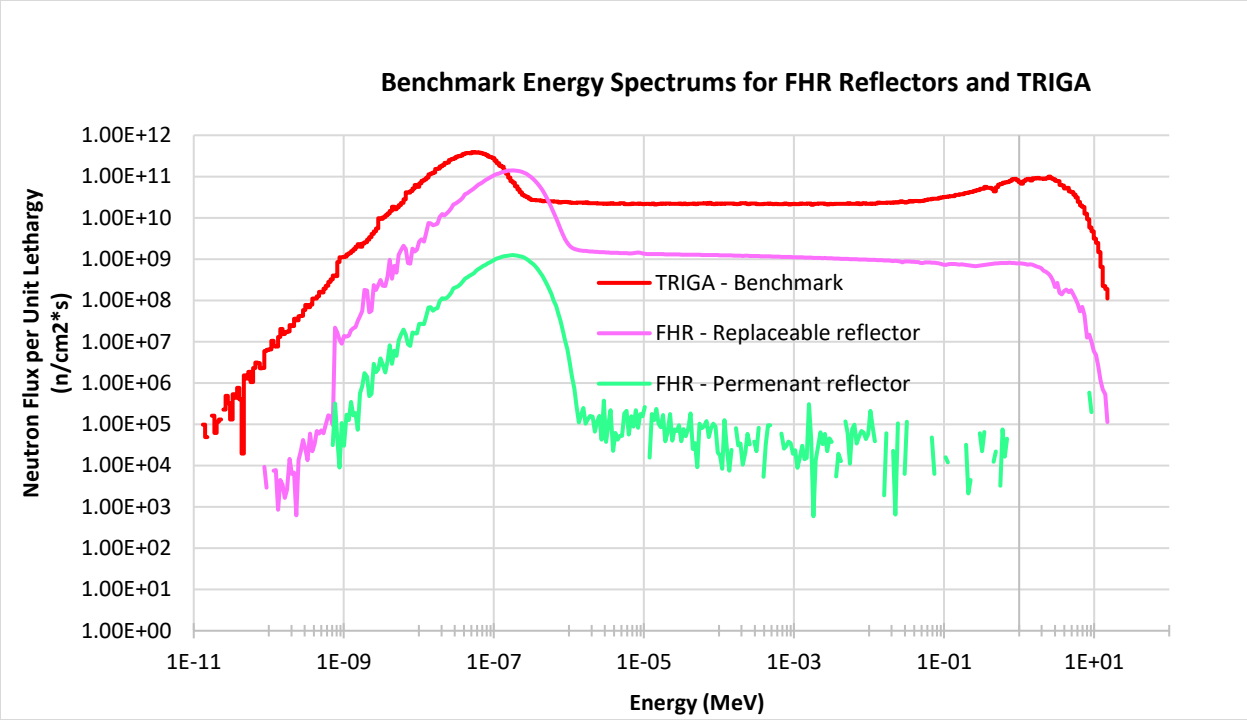

Figure 14: Benchmark energy spectrums for FHR reflectors and TRIGA

Table 5: Thermal Peak Energy of Benchmark Data for TRIGA and FHR

Comparison	Thermal Peak Energy (MeV)
TRIGA	5.06E-08
FHR Active Core	1.91E-07
FHR Flibe	1.66E-07
FHR Graphite	2.05E-07
FHR Reflectors	1.78E-07

Various Moderators in TRIGA

The first alteration tested various moderators and the effects of the energy spectrum in the D3 location. For this, commonly used moderators were selected: graphite, beryllium, and deuterium oxide (heavy water). In addition, a small flux trap consisting of TRISO fuel particles was placed in location D3 to determine whether the effects were worth researching further. Figure 23, located in the appendix, shows the data collected using various moderators in comparison to the original benchmark data of both the location D3 and the FHR locations of interest. The altered TRIGA spectrums were not comparable to the FHR because the thermal peak energy was not sufficiently close to the FHR data. The two energies were still a magnitude off from one another, so the comparison of temperatures ensued.

Various Graphite Temperatures in TRIGA

Due to the FHR's graphite moderator, the graphite simulations most accurately represented the FHR spectrum shape in all cases, thus it remained in the D3 location as the moderator for future simulations. Figure 24, located in the appendix, shows the TRIGA data with varying temperatures of graphite in the D3 location. The graphite spectrum magnitude is significantly lower than the TRIGA benchmark data with the thermal peak being five times less; however, the peak neutron energy shifted from the original TRIGA energy of 5.06E-8 MeV to anywhere between 1.26E-07 MeV $\leq E \leq$ 1.66E-7 MeV for the highest temperature of graphite at 2500 K. This value is incredibly high, but the central energy of the thermal peak is closer to all FHR thermal peak energies.

Various Absorbers in TRIGA

Absorption hardening is a phenomenon that occurs in reactors when absorbers are present. When neutrons are absorbed due to the presence of absorbers, the thermal peak shifts and centers over a higher thermal energy. This is because the lower energy neutrons are absorbed before

reaching those lower energies; therefore, the probability distribution of neutron energies shifts to a higher energy before the absorption energy. For these reasons, absorber materials were placed in the irradiation location to determine whether the absorption hardening affect was great enough to shift the TRIGA's spectrum to represent the FHR and VHTR.

For this research, two common thermal absorbers were used in simulations to determine the usability of the absorption hardening phenomenon: ^{10}B and ^{113}Cd. The graphite in location D3 was doped with 0.01% and 0.001% of both absorbers to determine their effectiveness. This is shown in Figure 25, and the thermal peaks did not shift enough to center around the FHR thermal energies.

Various Tally Locations in TRIGA

Since previous attempts did not shift the thermal peak energies enough, changing the location of the tally was tested. Locations D3, D2, and D1 (locations 1#, #2, and #3 respectively) are shown in Figure 15. Additional high-temperature graphite at 900 K and 2500 K was inserted into empty locations shown by turquoise blocks. This was done to better represent graphite-moderated cores. The results of these runs are shown in Figure 16 and Table 6.

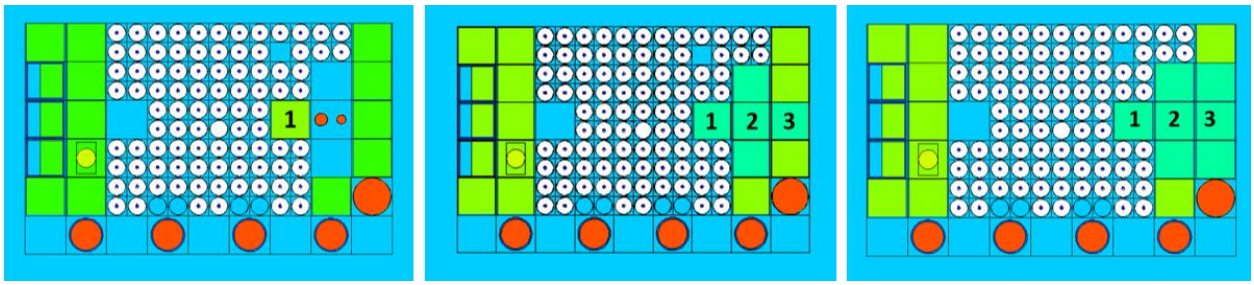

Figure 15: Top-down view of TRIGA reactor showing tally locations #2 and #3

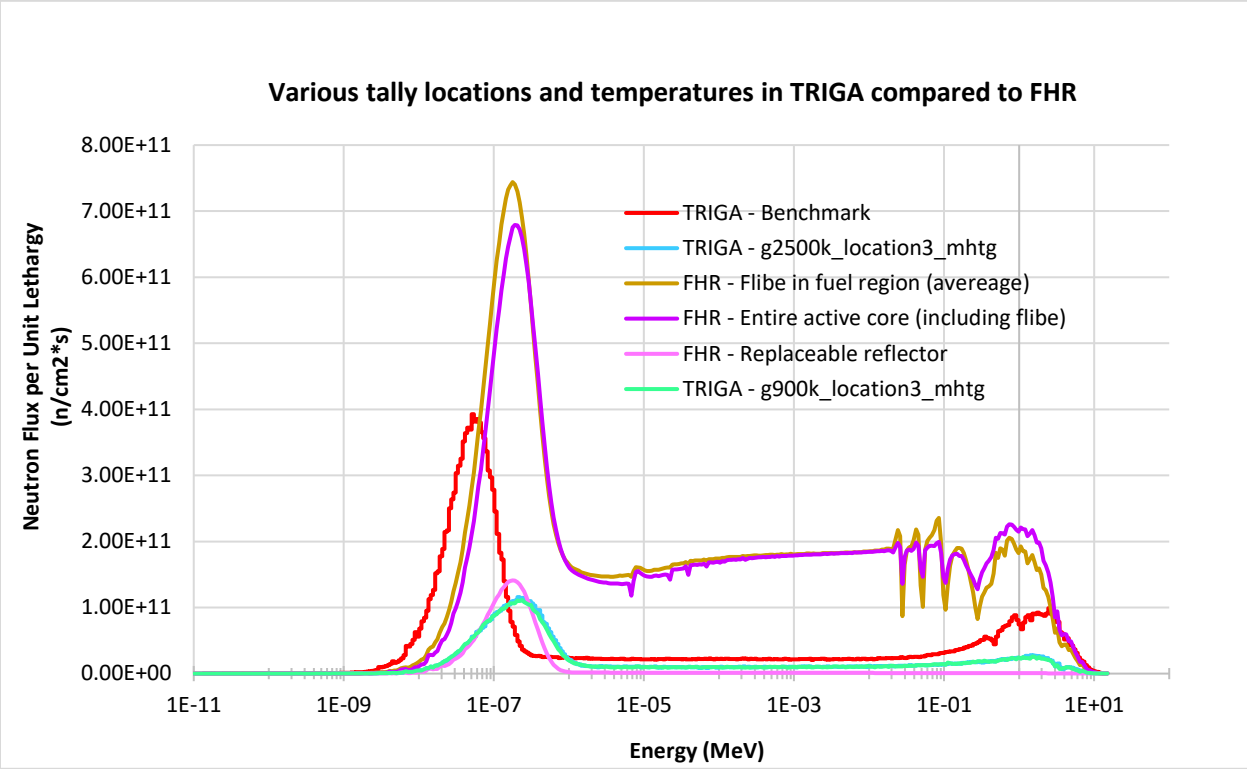

Figure 16: Best-comparison and physically realizable comparisons in TRIGA compared to FHR

Table 6: Thermal Peak Energies of Tallies Taken in Various Locations

Comparison	Thermal Peak Energy (MeV)
TRIGA g2500K Location #2	2.53E-07
TRIGA g2500K Location #3	1.78E-07
TRIGA g2500K Location #2 mhtg*	2.53E-07
TRIGA g2500K Location #3 mhtg	2.20E-07

*more high-temperature graphite

Comparing Table 5 and Table 6 reveal that tallying in D1 (location #3) at both 900 K and 2500 K most closely matches thermal energies with the FHR benchmark data in all cases (active core region, flibe, assembly graphite, and reflectors). From this, it is concluded that adding graphite and increasing the temperature of the graphite in an experimental setup will obtain the operating characteristics needed for FHR comparison. This is shown visually in Figure 16 where the peaks line up vertically. The 2500 K run in D1 lines up best with the FHR flibe and FHR reflectors while the 2500 K run with additional high-temperature graphite compares best with the FHR active core and FHR graphite comparisons. However, the 900 K run with additional high-temperature graphite is the best, physically realizable comparison. The centerline energy of this run is slightly higher than the true FHR comparisons, but the experimental setup can be adjusted to center around the corresponding centerline energies by either decreasing the amount of surrounding graphite or slightly decreasing the temperature. The best-comparison and best physically realizable simulations for the FHR locations of interest are shown concisely compared in Table 7.

Table 7: Benchmark data descriptions matched with best comparison and best physically realizable simulation between TRIGA and FHR

Comparison	Thermal Peak Energy (MeV)	Best Comparison	Thermal Peak Energy (MeV)	Physically Realizable Comparison	Thermal Peak Energy
FHR Active Core	1.91E-07	TRIGA g2500K Location #3 mhtg	2.05E-07	TRIGA g900K Location #3 mhtg	2.36E-07
FHR Flibe	1.66E-07	TRIGA g2500K Location #3	1.66E-07	TRIGA g900K Location #3 mhtg	2.36E-07
FHR Graphite	2.05E-07	TRIGA g2500K Location #3 mhtg	2.05E-07	TRIGA g900K Location #3 mhtg	2.36E-07
FHR Reflectors	1.78E-07	TRIGA g2500K Location #3	1.66E-07	TRIGA g900K Location #3 mhtg	2.36E-07

TRIGA and VHTR Comparison

The second comparison was between the TRIGA reactor and the VHTR reactor. The altered TRIGA spectrum for the VHTR was expected to be similar to the case required for the FHR due to the similarities between the FHR and VHTR fuel material, fuel design, and moderator choice. Figure 17 shows the TRIGA benchmark data compared to locations of interest in the VHTR reactor. The chosen regions were similar to the FHR; Tallies were taken over the entire active fuel region, the helium coolant, graphite in the active core region, and the graphite reflector. For this reactor, there was no distinction between a replaceable and permanent reflector in the MCNP file, so the entire reflector was tallied as one. As shown in Figure 17, the TRIGA spectrum is dwarfed by the spectrums of the VHTR. For this reason, the following VHTR spectrums will be represented at only 1.6% power (10 MWt) to allow better visual inspection.

According to Table 8, the thermal energies are similar in all cases for the VHTR. In fact, all energies are in bins directly adjacent to each other. Because all bins are adjacent, the middle energy can be used to represent all three peaks' centerline energy. This allows simple comparison of the TRIGA reactor to the VHTR considering only one region needs to be used as benchmark comparison. The centerline energy, 2.36E-7 MeV, in the VHTR active region graphite was chosen as the main benchmark data. This is because all other locations are closely relatable to the conclusions drawn from the VHTR graphite.

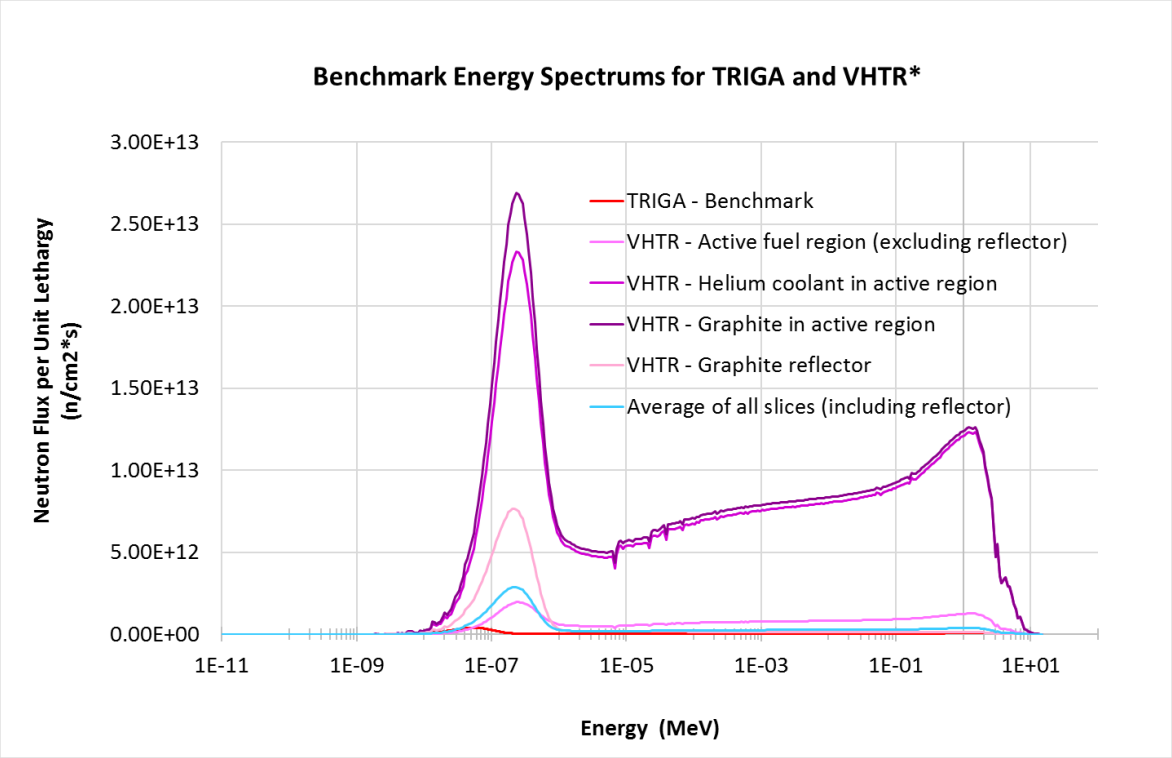

*VHTR at 600 MWt (100% power)

Figure 17: Benchmark energy spectrum for TRIGA and VHTR

Table 8: Thermal Peak Energy of Benchmark Data for TRIGA and VHTR

Comparison	Thermal Peak Energy (MeV)
VHTR Active fuel region	2.53E-07
VHTR Helium Coolant	2.36E-07
VHTR Graphite (active region)	2.36E-07
VHTR Reflector	2.20E-07
VHTR Average over entire core	2.20E-07

Various Moderators in TRIGA

Figure 27 shows the various moderators in the TRIGA reactor compared to the VHTR active core graphite. The results were equally as expendable as they were with the TRIGA versus FHR spectrums because the thermal peak energies did not sufficiently harden.

Various Graphite Temperatures in TRIGA

As with the FHR comparison, graphite remained the moderator of choice since it closely represents the shape of the VHTR spectrum in Figure 27. Various temperatures of graphite in the TRIGA were compared with the VHTR spectrum, and this comparison is shown in Figure 28. The thermal peaks have shifted significantly but are not representative of the VHTR spectrum, so other comparisons were made.

Various Absorbers in TRIGA

It was assumed that the presence of absorbers would not represent the VHTR since absorption hardening did not sufficiently shift the TRIGA spectrum to represent the FHR, and the VHTR spectrum is slightly harder than the FHR spectrum as shown in Figure 6. The comparative results are shown in Figure 29, and, as predicted, the TRIGA spectrum did not shift enough to accurately represent the VHTR.

Various Tally Locations in TRIGA

The same tally locations and data compared to the FHR were compared to the VHTR as well. Comparing the thermal energy peak data in Table 6 and Table 8, which is represented in Figure 18, shows a favorable comparison between the TRIGA peaks and the VHTR peaks. In the case of the TRIGA, the tally in D1 with more 900 K graphite best represents the VHTR thermal peaks. This comparison is consolidated in Table 9 where the center energy of 2.36E-7 MeV is directly relatable to the thermal peak energies of the TRIGA.

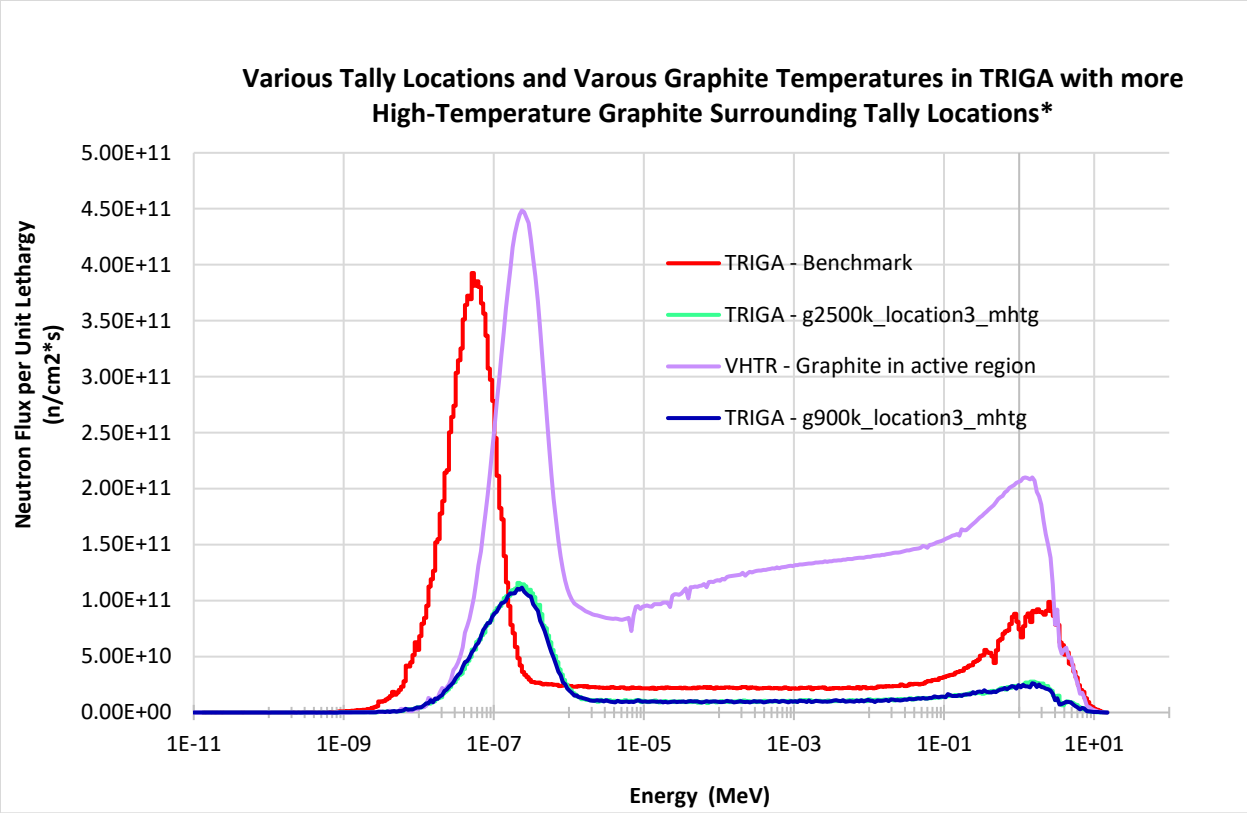

*VHTR at 10 MWt (1.6% power)

Figure 18: Best-comparison and physically realizable comparisons in TRIGA compared to VHTR

Table 9: Benchmark data descriptions matched with best comparison simulation between TRIGA and VHTR

Comparison	Thermal Peak Energy (MeV)	Comparison	Thermal Peak Energy (MeV)
VHTR Active fuel region	2.53E-07	TRIGA g900K Location #3 mhtg	2.36E-07
VHTR Helium Coolant	2.36E-07	TRIGA g900K Location #3 mhtg	2.36E-07
VHTR Graphite (active region)	2.36E-07	TRIGA g900K Location #3 mhtg	2.36E-07
VHTR Reflector	2.20E-07	TRIGA g900K Location #3 mhtg	2.36E-07
VHTR Average over entire core	2.20E-07	TRIGA g900K Location #3 mhtg	2.36E-07

Calculated FHR and VHTR Similarity Factors

The ratio of fluxes is a particular interest because it facilitates the conversion between TRIGA experimental results to FHR and VHTR predicted results. Figure 19 through Figure 21 show the similarity factors between the comparable TRIGA data and the FHR/VHTR regions of interest.

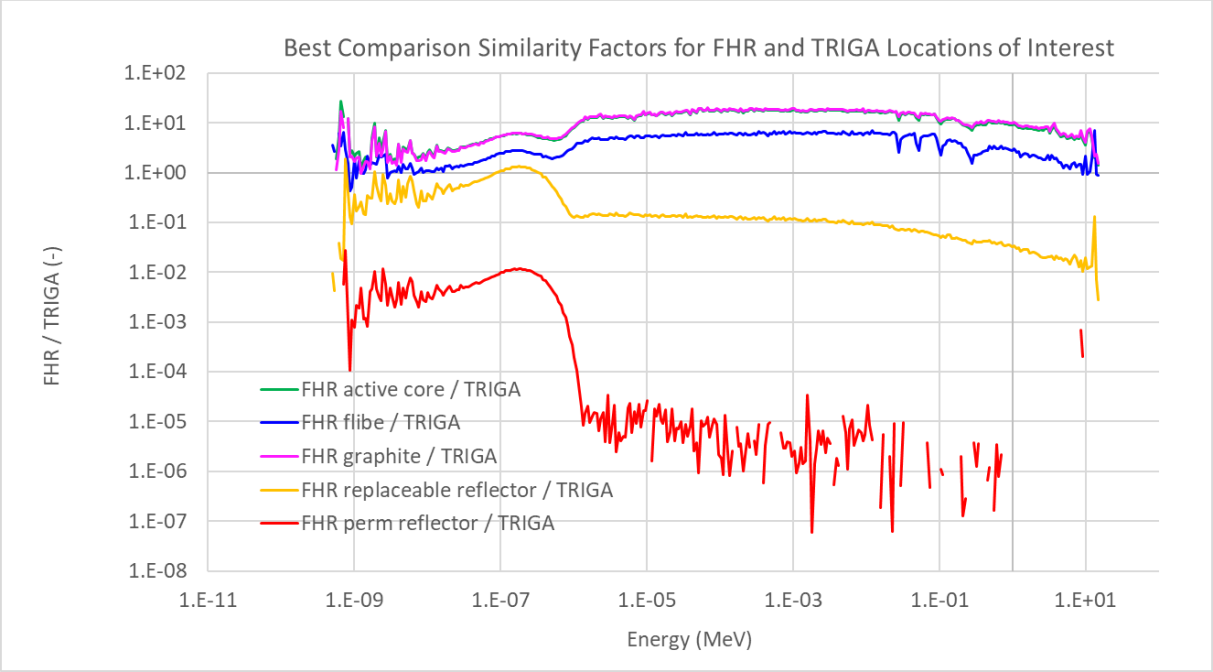

Figure 19: Best-comparison similarity factors for FHR and TRIGA

Figure 19 represents the best-comparison similarity factors for the FHR with and without the additional 2500 K graphite in D1. The spikes in the figures could be reduced by decreasing the relative flux errors. The lower and higher energy regions, where these spikes are shown, have relatively high errors where the majority fall between 30-40%, but the relative errors in the thermal

and epithermal regions were below 5%. In addition, the gaps in graph represent energies where the FHR tally was divided by a zero TRIGA tally. The spikes and data gaps are particularly noticeable in the very low and very high energy ranges because few, if any, neutrons of high and low energies were tallied. This is most apparent in the FHR's permanent reflector.

The highest similarity factor between the FHR and TRIGA is 19.9 while the lowest was far below one in the 1E-7 to 1E-8 range; however, the average of FHR/TRIGA similarity factors over all regions (excluding the permanent reflector) between $8.18E\text{-}8 \leq E \leq 1.30E1$ and without zero indices is about 6.47. (The permanent reflector was excluded in the average calculation due to the many zero indices.) The thermal region, where a factor of 20 is seen, has the largest similarity factors considering the great difference in the thermal peak heights especially when the FHR is at maximum operating power (600 MWt).

A similarity factor of about six is essentially showing that the difference in the neutron flux at this particular energy is about six times different. This is another way of saying the FHR flux is about six time higher than the TRIGA data at the given energy and thus, data for the FHR over a time period of one would have to be left in the TRIGA reactor for a time period of six to see comparable results. For this reason, a similarity factor of one is preferred considering it would show that results are equivalent and thus directly comparable. This is another reason for developing similarity factors; They allow the conversion of data when the spectrums are not exact both in shape and magnitude.

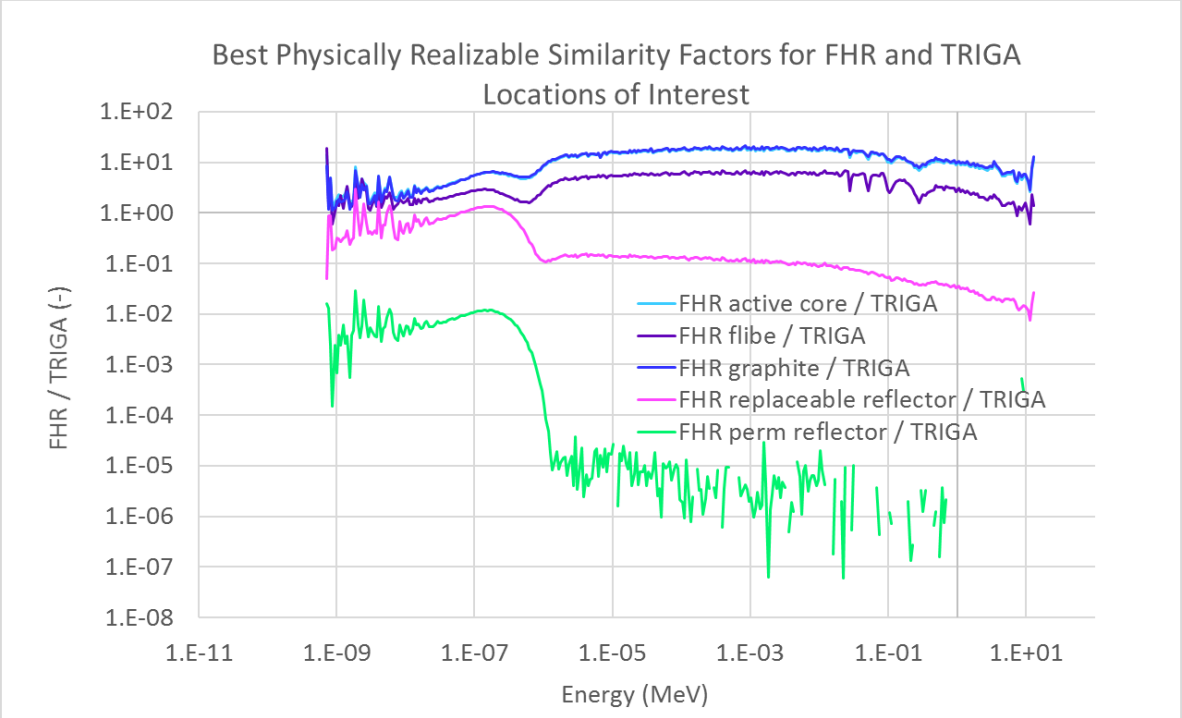

Figure 20: Physically realizable similarity factors for FHR and TRIGA

Figure 20 represents the most physically realizable similarity factors. While these results are not the best-fit to represent the FHR, 900 K is significantly more reasonable of a temperature for an experimental setup. In addition, the 900 K centerline energies are slightly higher than the true FHR energies, so the experimental setup can be altered slightly to represent both best-comparison and most physically realizable similarity factors. Most factors in all regions fall below 20 with the permanent reflector factors below one even in the thermal region. The average similarity factor over the same energies (once again excluding the permanent reflector similarity factors) is 6.60. This is only 2% different from the best-comparison average similarity factor thus validating that the physically realizable case can be used instead of the best-comparison case.

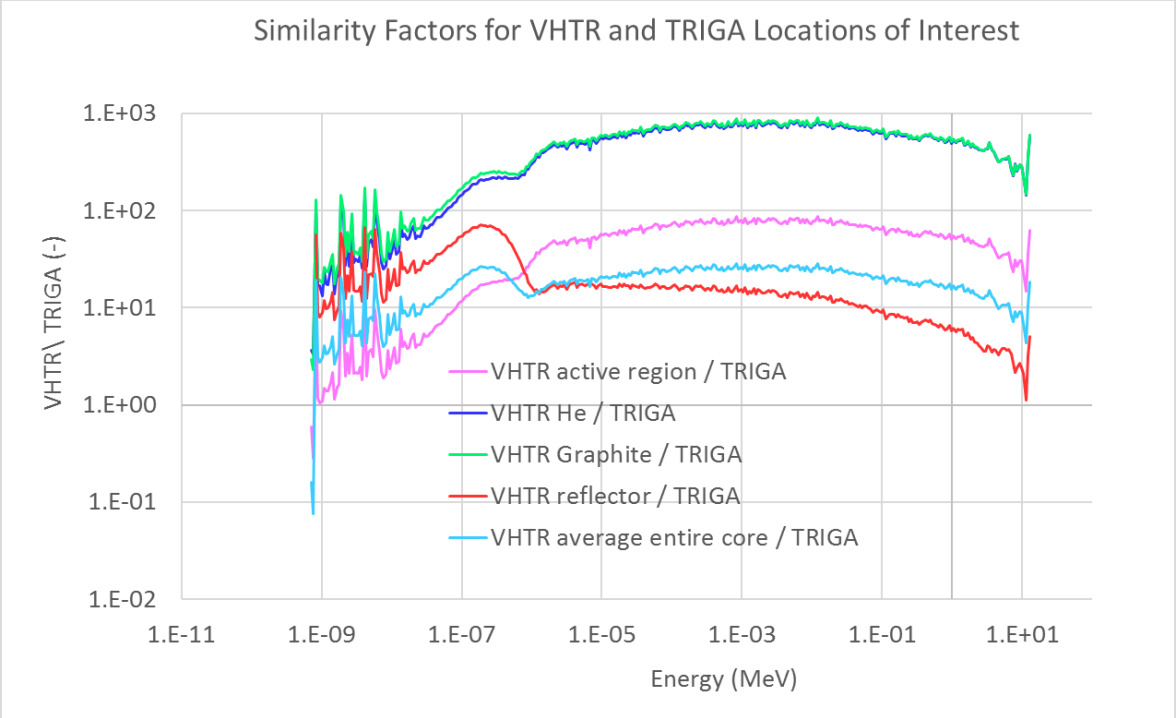

Figure 21: Best-comparison and physically realizable similarity factors for VHTR (600 MWt) and TRIGA

Both best-comparison and physically realizable reactor similarity factors for the VHTR are represented in a single figure, Figure 21, since they are the same. Firstly, the VHTR/TRIGA similarity factors are significantly higher than the FHR/TRIGA factors in all regions; however, the reflector and average over entire core have significantly smaller similarity factors because of the small neutron fluxes seen at the peripheral of the reactor core.

The highest similarity factor all of the regions is 880.19 which is located in the epithermal energy region and is significantly higher than any similarity factor found for the FHR core. The similarity factors for the VHTR were calculated with the core at full power (600 MWt) which aids to the significantly larger similarity factors. In addition, the average of all regions (taken over the

same energy ranges as the FHR factors) is about 203; however, this average includes all regions of interest in the VHTR (no reflector portion is excluded). Although the VHTR/TRIGA results are significantly higher than the FHR/TRIGA results, this does not present an issue because the similarity factors allow the comparison of spectrums that are not exact. To prove this concept, Table 10 has been included to demonstrate the similarity factor application at five energies. The original TRIGA, FHR, and VHTR data was presented along with the calculated similarity factors. Then the TRIGA data was multiplied by the similarity factor thus producing an FHR and VHTR corrected flux that represents the true FHR and VHTR original fluxes respectively. As shown, the corrected flux matches the original flux of interest.

Table 10: Similarity Factor Application Example

	TRIGA	FHR			VHTR		
Energy	900 K; D1	Entire Active Core			Active Fuel Region		
MeV	Original flux	Original flux	Similarity Factor	Corrected flux	Original flux	Similarity Factor	Corrected flux
1.55E-07	1.04E+11	6.47E+11	6.19	6.47E+11	1.61E+12	1.54	1.61E+12
1.66E-07	1.07E+11	6.61E+11	6.20	6.61E+11	1.69E+12	1.58	1.69E+12
1.78E-07	1.06E+11	6.75E+11	6.35	6.75E+11	1.77E+12	1.67	1.77E+12
1.91E-07	1.07E+11	6.79E+11	6.38	6.79E+11	1.83E+12	1.72	1.83E+12
2.05E-07	1.11E+11	6.78E+11	6.14	6.78E+11	1.88E+12	1.70	1.88E+12

TRIGA Burn Simulation

Experimental results depend on the TRIGA's neutronics consistency throughout the length of a given experiment. For these reasons, the TRIGA MCNP file was simulated at full power for two years to determine the criticality effects of the fission product buildup. Figure 22 shows the k_{eff} every 6 months (183 days) for a total of two years. The k_{eff} fluctuates, but the overall trend of the data is negative with respect to time. This makes sense since fuel is burned as the reactor is operating. The trendline falls within all error bars, which are based on the average standard deviation of all data points, thus validating the data, and the final k_{eff} falls within the error bars of the first k_{eff}. This means the final k_{eff} at the end of two years is statistically the same as the initial k_{eff}. This ultimately indicates that an experiment could run for two years while statistically maintaining consistent neutronics characteristics in the TRIGA core.

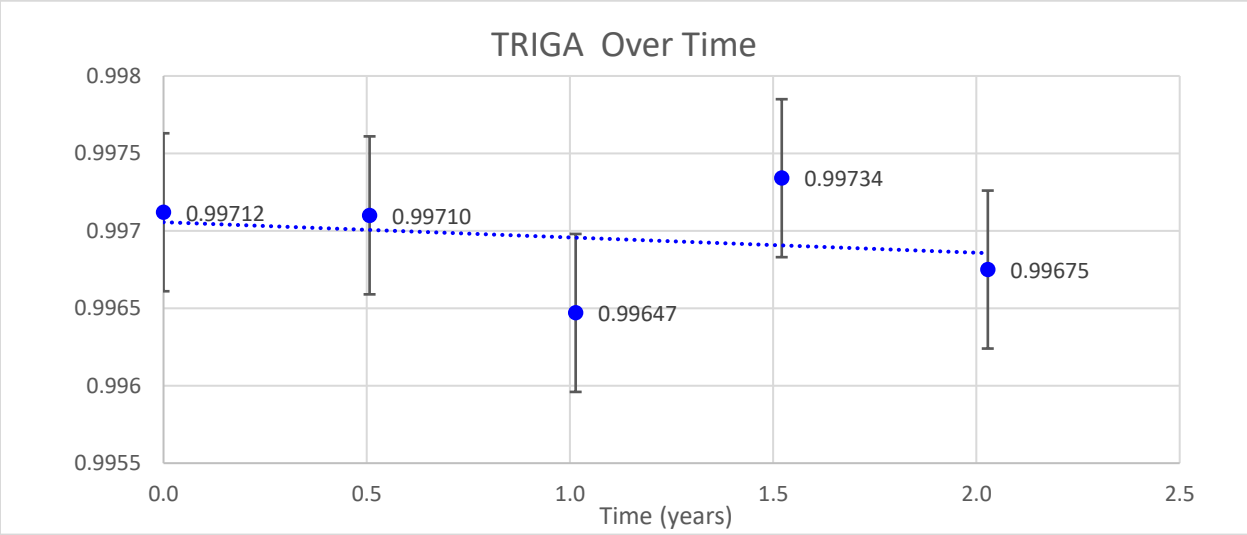

Figure 22: TRIGA k_{eff} changes over two years of full-power operation

CONCLUSIONS

The advancement of generation IV reactors depends on experiments proving advanced equipment resistance to advanced operating conditions. Due to the extreme conditions, these experiments become increasingly important and difficult to complete. This report analyzed the ways that currently operating research reactors can progress the theoretical challenges and eventually aid the experiments that will progress generation IV reactors off paper and into production.

Texas A&M's TRIGA reactor can be used for such experiments given the nature of the reactor's core design, and it will provide adequate and consistent neutronics (for at least two years) at a reasonable price compared to national laboratory reactors. However, the TRIGA reactor must be altered to represent the FHR and VHTR properly. The data shows that the addition of high-temperature graphite, both at 900 K and 2500 K, in the TRIGA's D1 and D2 locations can adequately represent the FHR and VHTR thermal peak operating conditions. The reactor physics similarity factors calculated from the best and most physically realizable results will facilitate converting experimental results into useful data. This will aid in determining the strenuous operating environment equipment for advanced reactors will see.

It is important to note that the k_{eff} of the TRIGA reactor was not drastically altered by the addition of 900 K graphite into the core. The k_{eff} values of the original benchmark data and the altered TRIGA can be seen in Table 11. Assuming the benchmark data is the actual data, the k_{eff} was altered by only 1.1%. If this is determined to be too large of an alteration, neutron absorbers doped into the graphite blocks could provide a solution. Given the calculated similarity factors and the

collected data, this research will help progress the understanding of advanced reactor equipment resistance in extreme operating conditions.

Table 11: TRIGA k_{eff} values before and after addition of 900 K graphite

	Original (Benchmark)	Altered
k_{eff}	0.99709	1.00774
1σ	0.00044	0.00047
Difference	1.1%	

Even though there already exist promising outcomes, there are additional elements that could be included and others to be improved that would further develop this research. These elements are expressed below.

- FHR future research elements
    - Find energy spectrum in other parts of the MCNP model—to determine equipment resistance and data collecting accuracy in these locations over the lifetime of the reactor.
- VHTR future research elements
    - Build upon the current MCNP model and find the energy spectrum in other areas for the same reasons presented above;
    - Determine energy spectrum in upper and lower graphite reflectors—this will be important for research development considering graphite's sensitivity to radiation embrittlement and the necessary data collection to monitor such embrittlement;
    - Distinguish the replaceable and permanent reflector and determine energy spectrum—this is also important because of radiation embrittlement.

- TRIGA future research elements
    - Examine the energy spectrums outside of TRIGA core as potential irradiation locations.

Incorporating the information from these elements will further the development of both the FHR and VHTR. Using the presented similarity factors as conversion factors, experiments completed in the TRIGA reactor can adequately represent the conditions that would be seen in an advanced reactor design.

REFERENCES

[1] "Thorium," World Nuclear Association, February 2017. [Online]. Available: http://www.world-nuclear.org/information-library/current-and-future-generation/thorium.aspx. [Accessed 2017].

[2] "JANIS (Java-based Nuclear Data Information System)," Nuclear Energy Agency, 2013.

[3] K. A. P. Laboratory, *Chart of the Nuclides: 17th Edition*, 2016.

[4] C. Forseberg, "The Advanced High-Temperature Reactor: HIgh-Temperature Fuel, Liquid Salt Coolant, Liquid-Metal-Reactor Plant," Elsevier Ltd. , Amsterdam, 2005.

[5] J. W. Sterbentz, R. L. Sant, P. D. Bayless and R. R. Schultz, "NGNP Preliminary Point Design - Results of the Initial Neutronics and Thermal-Hydraulic Assemssments," Idaho National Engineering and Enviromental Laboratory, Idaho Falls, 2003.

[6] "TRIGA Reactor," Texas A&M Engineering Experiment Station, 2017. [Online]. Available: https://nsc.tamu.edu/about-the-nsc/triga-reactor/. [Accessed 2017].

[7] X.-5. M. C. Team, *MCNP - A General Monte Carlo N-Particle Transport Code, Version 5 Volume 1: Overview and Theory*, Los Alamos, 2003.

[8] T. V. Hung, Y. Sakamoto and H. Yasuda, "Calculations of Neutron Flux Characteristics of Dalat Reactor using MCNP4A Code," Japan Atomic Energy Research Institute, 1998.

APPENDIX

TRIGA and FHR Comparison Spectrums

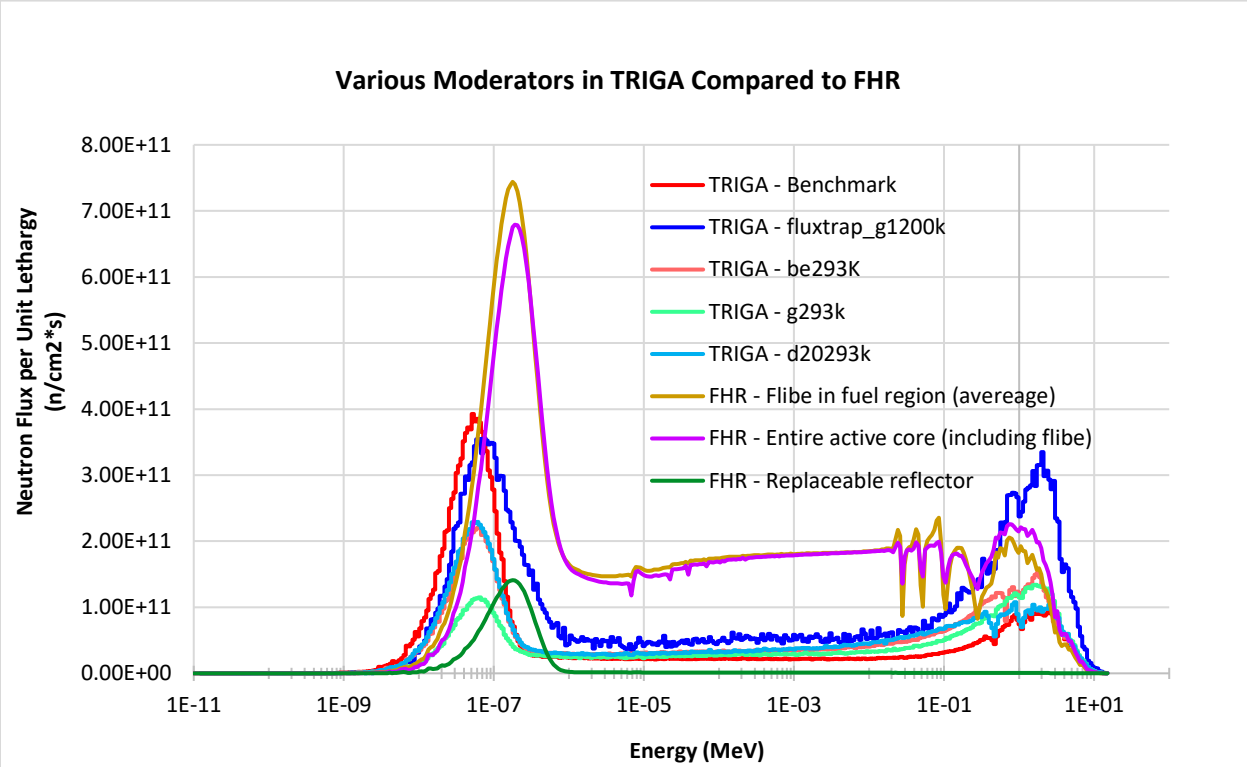

Figure 23: Various moderators in TRIGA compared to FHR

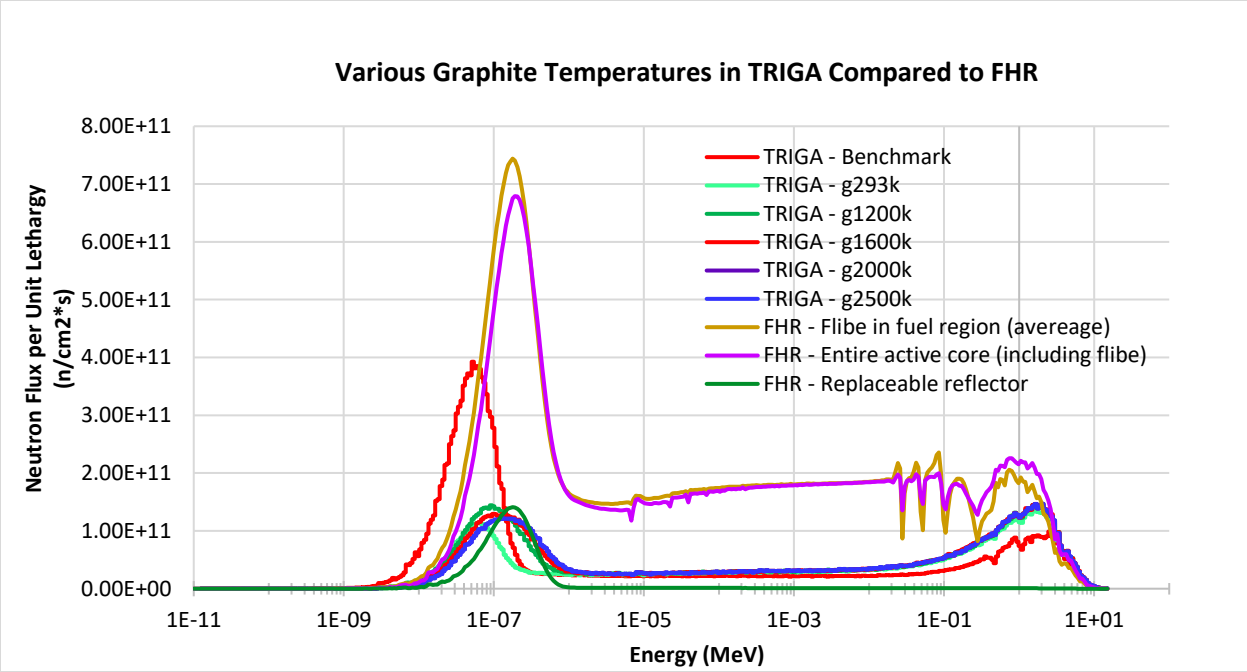

Figure 24: Various graphite temperatures in TRIGA compared to FHR

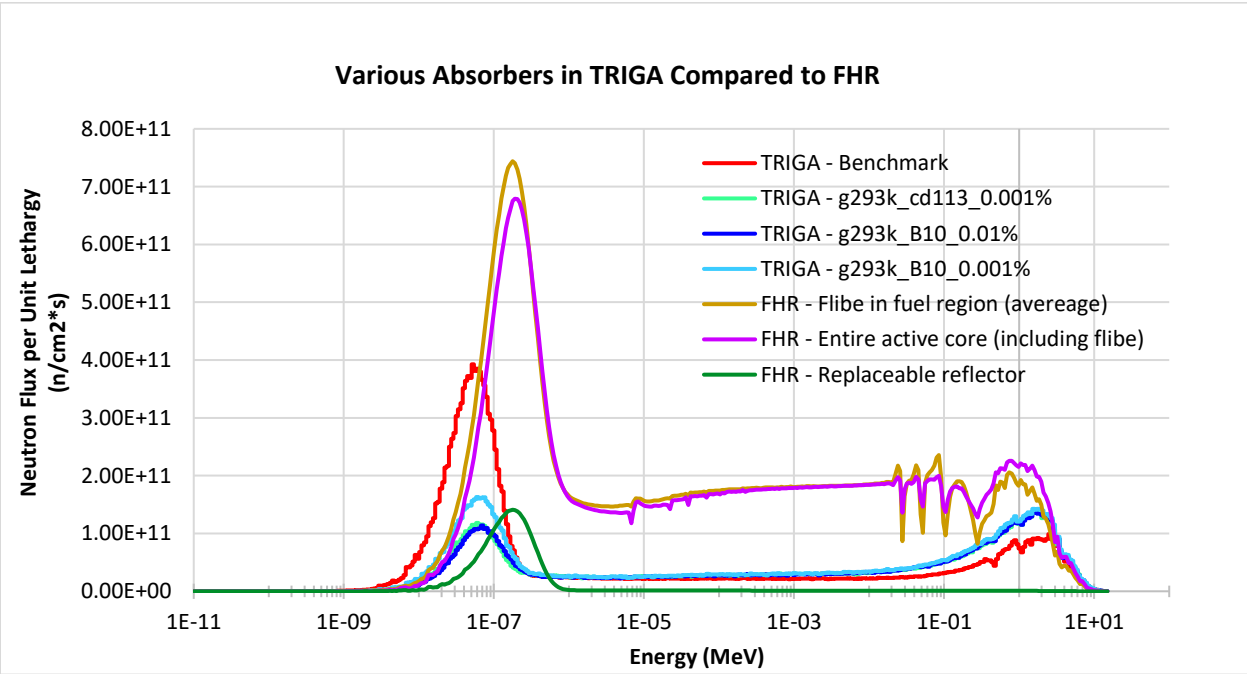

Figure 25: Various absorbers in TRIGA compared to FHR

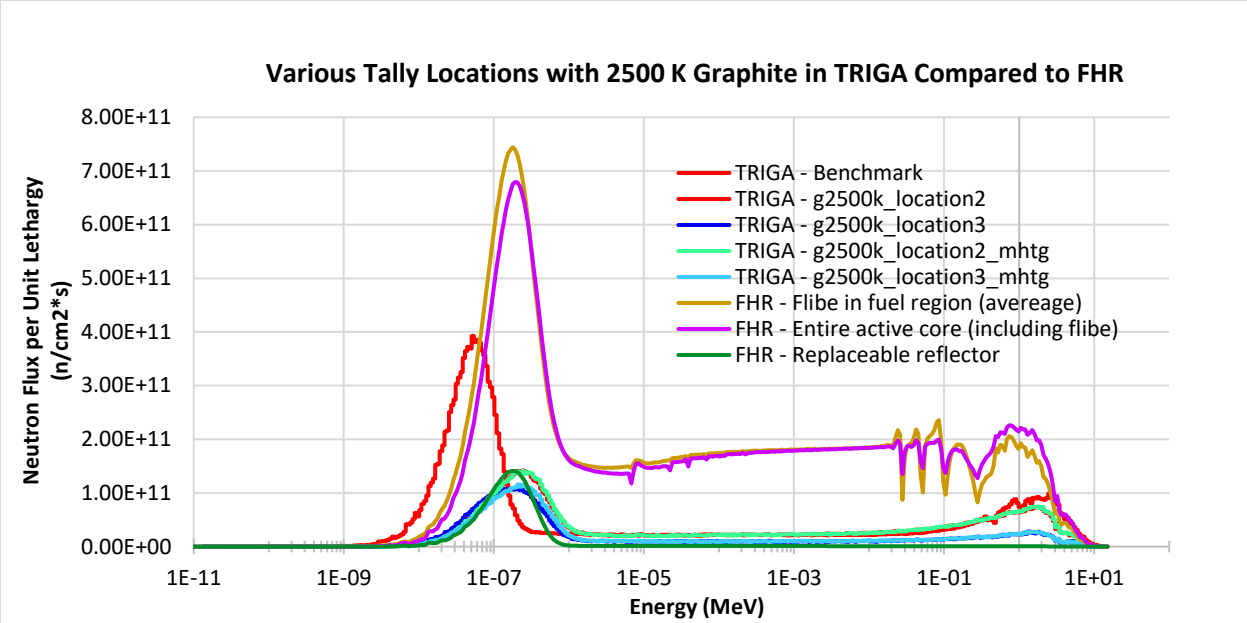

Figure 26: Various tally location with 2500K graphite in TRIGA compared to FHR

TRIGA and VHTR

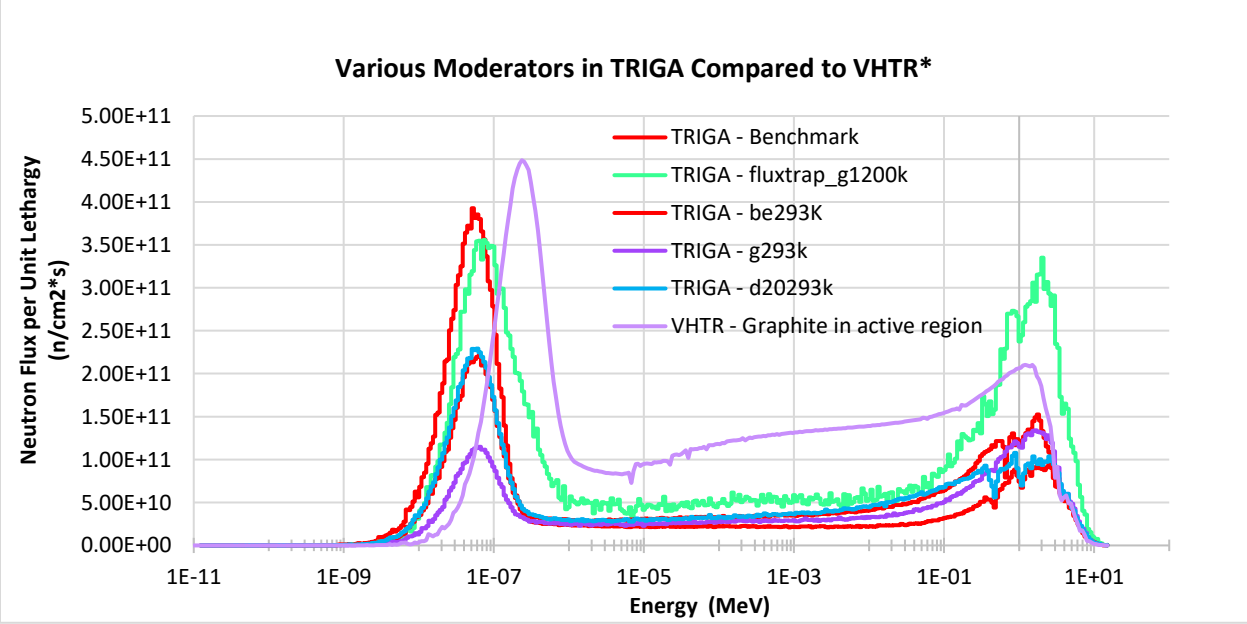

*VHTR at 10 MWt (1.6% power)

Figure 27: Various moderators in TRIGA compared to VHTR

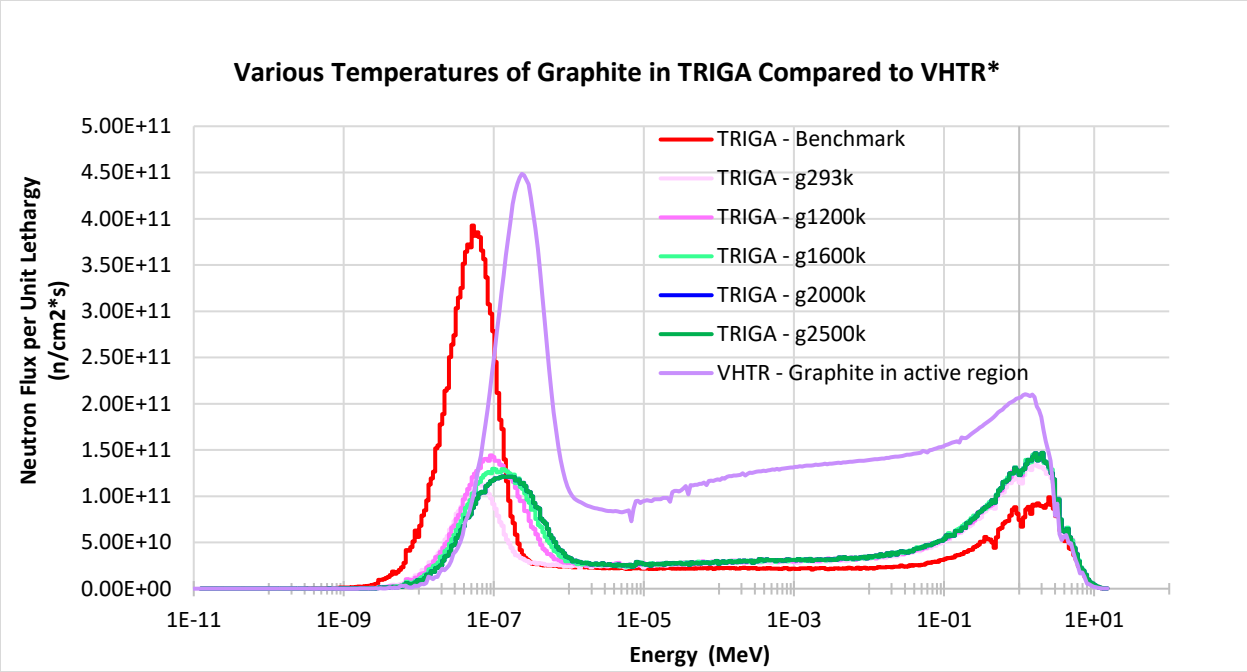

*VHTR at 10 MWt (1.6% power)

Figure 28: Various temperature of graphite in TRIGA compared to VHTR

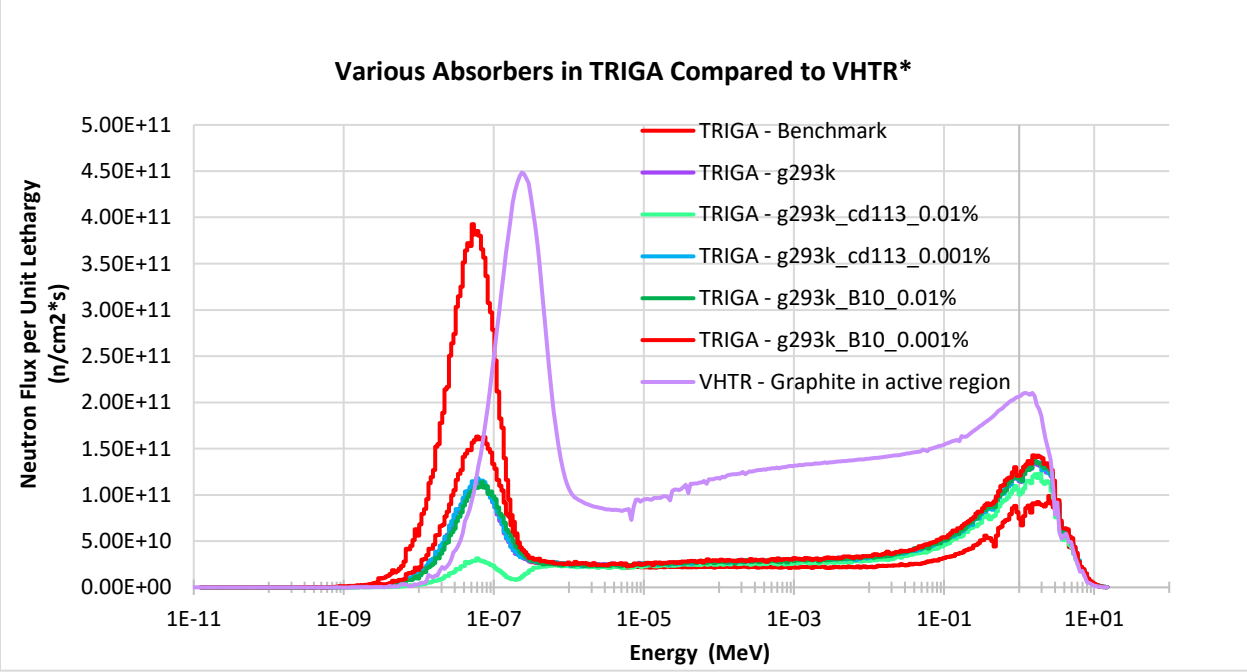

*VHTR at 10 MWt (1.6% power)

Figure 29: Various absorbers in TRIGA compared to VHTR

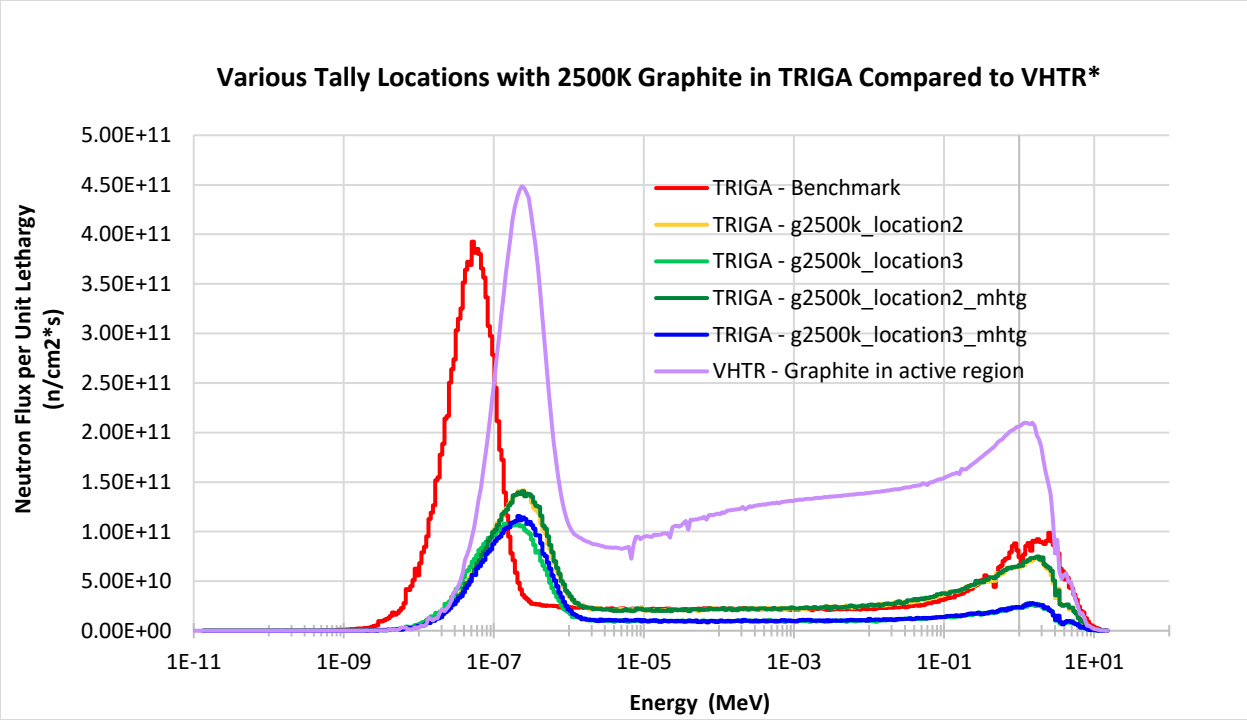

*VHTR at 10 MWt (1.6% power)

Figure 30: Various tally locations with 2500K graphite in TRIGA compared to VHTR